The geochemical behavior of Cu and its isotopes in the Yangtze River

Qian Wang[a], Lian Zhou[a]*, Susan H. Little[b], Jinhua Liu[a], Lanping Feng[a], Shuoyun Tong[a]

[a]*State Key Laboratory of Geological Processes and Mineral Resources, China University of Geosciences, Wuhan 430074, China*

[b]*Department of Earth Sciences, University College London, Gower Street, London WC1E 6BT*

*Corresponding author

Lian Zhou (e-mail: zhcug@163.com)

State Key Laboratory of Geological Processes and Mineral Resources.

China University of Geosciences, Wuhan 430074, China

Graphical abstract:

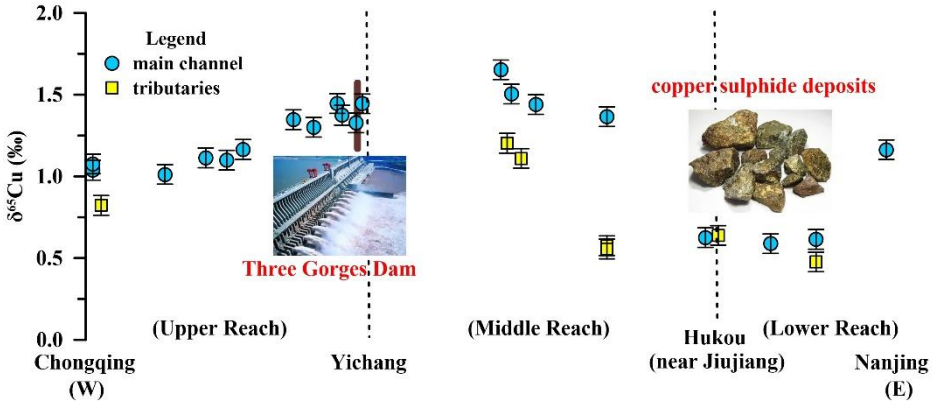

Abstract:

Copper (Cu) isotopes can be a useful tool to constrain the interaction of water and the environment, but they have not been widely applied to riverine research in the preceding decades. Isotopically heavy Cu in rivers (global average: about +0.7‰) compared to rocks (at about 0‰) has been attributed to: a) the mobilization of heavy Cu during oxidative weathering, and b) partitioning between an isotopically heavy, organically complexed dissolved pool, and an isotopically light pool adsorbed to particulates. Here, we report Cu concentrations and isotope ratios of the main stream of the Yangtze River and its several tributaries. We find that the Yangtze River exhibits anomalously heavy Cu isotope compositions compared to other rivers: $\delta^{65}Cu_{NIST\ 976}$ of dissolved Cu for the main stream, from Chongqing to Nanjing, ranges from +0.59 to +1.65‰, while the tributaries vary from +0.48 to +1.20‰. A negative correlation is observed between Cu concentrations and Cu isotope compositions.

We attribute the anomalous Cu isotope geochemistry of the Yangtze River to two key features of the basin: first, the influence of the Three Gorges Dam (TGD), and second, the presence of extensive Cu sulphide deposits close to the lower reaches of

the river. In the upper reaches, downstream towards the TGD, δ^{65}Cu values increase as Cu concentrations decrease, reflecting the preferential adsorption of light Cu by sedimenting particulate phases. δ^{65}Cu values continue to increase to a maximum of +1.65‰ in the middle reaches, at Guangxingzhou. The lower reaches, from Jiujiang to Tongling, are characterized by less positive values of δ^{65}Cu (at about +0.60‰), due to the oxidative weathering of Cu sulphide deposits. The overall Cu-δ^{65}Cu trend in the river reflects mixing of these waters from the lower reaches, influenced by Cu sulphides, with waters from upstream, which have lower Cu concentrations and elevated δ^{65}Cu values.

Keywords: Yangtze River; Cu isotopes; Three Gorges Dam; Cu sulphide deposits

1. Introduction

Copper has two stable isotopes, ^{63}Cu and ^{65}Cu, and is a principal metal in ore-forming processes. Copper isotopes may be a useful tool to trace the fate of Cu during long-term geological processing, and to shed light on its biogeochemical cycling in the natural environment (Zhu et al., 2000; Larson et al., 2003; Weinstein et al., 2011). In recent years, the application of multi collector inductively coupled plasma mass spectrometry (MC-ICP-MS) has brought a great improvement in the determination of Cu isotope ratios (Maréchal et al., 1999; Bermin et al., 2006), and Cu isotopes are increasingly being applied in the fields of geology, biology and environmental sciences (Moynier et al., 2017).

Recent work on Cu isotopes in rivers and the oceans has demonstrated that

dissolved Cu (+0.02 to +1.45‰) is isotopically heavy compared to the solid Earth (about 0‰) (Vance et al., 2008; Takano et al., 2014; Little et al., 2018). Several possible mechanisms to explain this phenomenon have been suggested.

First, isotopically light Cu may be preferentially adsorbed by clay and oxy(hydr)oxide minerals, either during weathering (Vance et al., 2016; Guinoiseau et al., 2017; Kusonwiriyawong et al., 2017; Little et al., 2019) or via scavenging of Cu from the aqueous phase (Takano et al., 2014). Laboratory sorption experiments indicate that light Cu isotopes are preferentially adsorbed onto kaolinite (Li et al., 2015) and Mn oxides (Ijichi et al., 2018), though heavy isotopes tend to be adsorbed onto iron oxy(hydr)oxide surfaces (Balistrieri et al., 2008; Pokrovsky et al., 2008). In addition, bacteria-metal interaction experiments indicate that live bacteria cells preferentially take up the lighter Cu isotope regardless of the experimental conditions (Navarrete et al., 2011).

Second, organic complexation dominates the speciation of Cu in rivers and oceans (Vance et al., 2008; Takano et al., 2014; Thompson et al., 2014; Thompson and Ellwood, 2014; Little et al., 2018; Baconnais et al., 2019) and organic ligands preferentially complex isotopically heavy Cu in the dissolved phase (Ryan et al., 2014). Dead bacterial surfaces preferentially adsorb the heavier Cu isotope, which likely reflects fractionation due to complexation with organic acid surface functional group sites (Navarrete et al., 2011). During weathering, organic complexation of the heavier Cu isotope has been proposed as one mobilization mechanism for Cu (Bigalke et al., 2011; Vance et al., 2016; Little et al., 2019).

Third, the oxidation (or reduction) of Cu can also lead to isotope fractionation. Oxidised Cu^{2+} species will tend to accumulate heavy Cu isotopes, while reduced Cu^{+} species will be isotopically light (Ehrlich et al., 2004; Asael et al., 2007; Fujii et al., 2013, 2014; Sherman, 2013). The abiotic fractionation of Cu in Cu sulphide-rich ore deposits is associated with the preferential oxidation of $^{65}Cu^{+}$ at the mineral surface and the formation of an isotopically heavy oxidized layer (Kimball et al., 2009). This layer is then leached during further weathering, releasing heavy Cu to the dissolved phase. It has been documented that leachate Cu solutions derived from sulphides such as chalcopyrite (Mathur et al., 2005; Fernandez and Borrok, 2009; Kimball et al., 2009), chalcocite (Mathur et al., 2005), bornite (Wall et al., 2011), and enargite (Kimball et al. 2009) have $\delta^{65}Cu$ values that range from +1.0 to +3.5‰ relative to the initial sulphide (Mathur et al., 2014; Song et al., 2016).

Extensive studies on the geochemistry, hydrology and environment of the Yangtze River have been carried out for more than 140 years (Zhang et al., 1998; Chen X. et al., 2001; Du et al., 2001; Chen et al., 2002; Ding et al., 2004, 2014; Chetelat et al., 2008, 2009, 2013; Wu et al., 2013; Zhang et al., 2014; Wang et al., 2015). Several studies have demonstrated that the Three Gorges Dam (TGD) has led to many changes to the environment of the Yangtze River and surroundings (Xu and Milliman, 2009; Li et al., 2011; Guo et al., 2012; Luo et al., 2012). To date, some Cu isotope data have been presented for the Yangtze River at Wuhan (Vance et al., 2008), showing that the $\delta^{65}Cu$ of the Yangtze River is anomalously positive compared to other global rivers, which have a general tendency towards lower dissolved Cu

concentrations for heavier dissolved Cu isotope compositions. Here, we present a more comprehensive Cu isotope dataset for the Yangtze River and its tributaries, which provides useful information to help understand the geochemical behavior of Cu and its isotopic fractionation during weathering and in the aqueous environment.

2. Methodology

2.1. Geological setting

The Yangtze River is the third-largest river in the world and plays an important role in human society, such as freshwater supply, transportation, flood prevention, and electricity. The Yangtze River, with a length of about 6300 km, lies between 90°33′-122°25′ E and 24°30′-35°45′ N and covers a total area of 1.81×10^{6} km^{2} (Chen X. et al., 2001; Chen et al., 2002). According to hydrologic and geographic conditions, the Yangtze River can be divided into three sections (Fig. 1): the upper reaches, from river source to Yichang (CJ-30); the middle reaches, from Yichang (CJ-30) to Hukou (near JJ-1); and the lower reaches, from Hukou (near JJ-1) to the East China Sea (Chen Z. et al., 2001).

The Yangtze River is situated in a subtropical monsoon climate region and the annual precipitation of most areas through which it flows ranges from 800 to 1600 mm (Ding et al., 2013). The drainage basin encompasses a very diverse range of rock types, which is mainly overlain by sedimentary rocks composed of marine carbonates, evaporites and alluvium from Precambrian to Quaternary age (Chetelat et al., 2008; Ding et al., 2014). Carbonate rocks are widely spread throughout the basin and are

124 particularly abundant in the southern part (Yunnan, Guizhou and western Hunan
125 Provinces) and the sub-basin of the Hanjiang (Chen et al., 2002; Chetelat et al., 2009).
126 Clastic rocks are mainly found in the upper reaches (Fig. 1).

127 The Yangtze River flows from the Qinghai-Tibet Plateau to the East China Sea
128 and passes through the Three Gorges Dam (TGD) at Yichang city, Hubei province
129 (Chen et al., 2002). The intercept of the TGD has affected the Yangtze River discharge,
130 which caused a decrease in sediment supply to the East China Sea (Chen et al., 2008;
131 Li et al., 2011; Guo et al., 2012; Luo et al., 2012).

132 **2.2. Sampling and analytical methods**

133 Samples from Wuhan to Nanjing (the main channel and associated tributaries)
134 were collected during September 2013, and samples from Chongqing to Chibi (the
135 main channel and associated tributaries) were collected at the end of July 2014 (Fig.
136 1). The average annual precipitation and discharge of the Yangtze River basin in 2013
137 were 1029.6 mm and 27506.7 m^3/s. In 2014, the average annual precipitation was
138 1100.6 mm and the average discharge was 31774.2 m^3/s (data from the Changjiang &
139 Southwest Rivers Water Resources Bulletin), with no significant differences of the
140 precipitation and discharge from 2013 (7% and 15%, respectively). The climate of the
141 Yangtze River basin is rainy and hot in both July and September (Changjiang &
142 Southwest Rivers Water Resources Bulletin). Therefore, the two datasets we collected
143 are comparable and can be discussed together. The vertical heterogeneities are present
144 in the river sections (Bouchez et al., 2010; Guinoiseau et al. 2016), and we only
145 collected surface water samples in this study. Samples were collected by boat, distally

146 from the riverbank. A long (approx. 15 m) rope was attached to the sampling bottle to
147 collect samples (2-4 L) as great a distance from the bow of the boat as possible. The
148 water samples were collected in pre-cleaned plastic bottles (PP) that were leached
149 with ultra-pure HCl (1 M) for 48 h, and then rinsed four times with Milli-Q water.
150 Clean bottles were rinsed twice with ambient river water before final collection of
151 water samples. The pH, electrical conductivity (EC) and dissolved oxygen (D.O.)
152 were measured using a Multi-3410 portable multiparameter digital dual input analyzer
153 (Table 1).

154 All indoor work was carried out under "class 100" laboratory conditions and all
155 reagents were purified in-house prior to use. Within 5 days of collection, samples
156 were filtered through 0.22 μm cellulose acetate filter membranes by SHZ-D（Ⅲ）
157 SHB-3 Water Circulating Vacuum Pump. These <0.22μm filtered water samples are
158 referred to as "dissolved" (they may contain some colloidal material). Filtered
159 samples were then acidified to pH < 2.5 using double sub-boiling distillation
160 concentrated HNO_3. About 250 mL of each was evaporated to dryness on a hot plate
161 at 100°C. After that, 2-3 mL 8.5 M HCl + 0.03% H_2O_2 was added and samples
162 evaporated to dryness once more, to convert all cations to chloride species. The final
163 dry residues were redissolved in 1 mL 8.5 M HCl + 0.03% H_2O_2 for the purification
164 of Cu using the AG MP-1M anion exchange resin (Bio-Rad, 100-200 mesh) (Hou et
165 al., 2016), which followed a modified protocol from Maréchal et al. (1999). The total
166 procedural blank of the process was <1.0 ng, accounting for less than 1.0% of the Cu
167 concentration of our measured solution samples. A further 50 mL of each filtered

water sample was dried down to analyze Sr isotope ratios. The Sr separation from major elements for isotopic analysis was carried out using an AG50W-X8 cation exchange resin (Bio-Rad, 200-400 mesh) and 2.5 M HCl (1 mL for load, 18.6 mL for rinse, 12 mL for elute) (Hans et al., 2013). The pure Sr solutions were then evaporated to dryness to be measured.

All samples were analyzed for major element (Na, Mg, Ca) and trace element concentrations by Inductively Coupled Plasma Mass Spectrometry (ICP-MS) (Agilent Technologies 7700 series) in the State Key Laboratory of Geological Processes and Mineral Resources (GPMR), Wuhan, China. Indium was used as an internal standard to correct for instrumental drift and eventual matrix effects. The ICP-MS internal precision was generally lower than 2% for most of the elements, the Cu detection limit was 1 nmol/L and the relative standard deviation (RSD) was lower than 5%.

Copper isotope compositions were measured at GPMR using a Multiple Collector Inductively Coupled Plasma Mass Spectrometer (MC-ICP-MS) (Neptune Plus, Thermo Finnigan Scientific, Bremen, Germany). The samples were introduced using a conventional system that consists of a tandem quartz spray chamber (cyclone + standard Scott double pass) coupled with a low flow PFA nebulizer (50 μL/min). We measured Cu isotope ratios in low-resolution mode and used a combined standard sample bracketing and internal normalization method (C-SSBIN) with Ga addition to correct mass bias. More details are given in Hou et al. (2016).

Copper isotope compositions are reported relative to the NIST SRM 976 standard. Delta per mil (‰) notation for the Cu isotope ratio is employed as follows:

$$\delta^{65}\mathrm{Cu} = \left(\frac{R_{sample}}{R_{standard}} - 1\right) \times 1000 \quad (1)$$

In this equation, R_{sample} and $R_{standard}$ represent the measured $^{65}Cu/^{63}Cu$ ratios of sample and NIST SRM 976 standard, respectively. As we were not able to duplicate all the samples, the error of 0.06‰ given is an external reproducibility obtained on the repeated analysis of several USGS reference materials from the GPMR MC-ICP-MS. The $\delta^{65}Cu$ for three USGS reference materials are reported in Table 2. Values for BHVO-2, BCR-2 and GSP-2 fall within the ranges recommended in Moynier et al., (2017) and Liu S. et al., (2014).

Strontium isotopes were measured at GPMR using a Thermal Ionisation Mass Spectrometer (TIMS) (Triton, Thermo Finnigan Scientific, Bremen, Germany). The long-term measured value of NIST 987 standard was $^{87}Sr/^{86}Sr$ = 0.71024 ± 0.00001 (2σ, n≥50), which was in good agreement with the given value of 0.71023 ± 0.00001 (Wang et al., 2007). The value of procedural standard "BCR-2" was $^{87}Sr/^{86}Sr$ = 0.705019 ± 0.000009 (2σ), which corresponds with the reference value of 0.705015 ± 0.000013 (Balcaen et al., 2005).

3. Results

The pH of the water samples ranges from 7.37 to 8.36 and dissolved oxygen (D.O.) from 5.06 to 8.64 mg/L. The electrical conductivity (EC) of the main stream ranges from 274 to 404 $\mu S \cdot cm^{-1}$, while the tributaries have a wider range of 148 to 709 $\mu S \cdot cm^{-1}$. The concentrations of Ca and Mg in the Yangtze River main stream water range from 833 to 1225 μmol/L and 304 to 490 μmol/L, respectively, with decreasing trends from the upper to lower reaches (Fig. 2). The main stream water of

the Yangtze River has considerably higher Sr concentrations (1924 to 4865 nmol/L) and slightly lower $^{87}Sr/^{86}Sr$ isotopic ratios (0.709923 to 0.711139) (Table 1) than the global average river values of dissolved Sr (890 nmol/L) and $^{87}Sr/^{86}Sr$ isotopic ratio (0.7119) (Palmer and Edmond, 1989), consistent with the data of Wang et al. (2007).

The Cu concentration of the main stream and tributaries ranges from 16.0 to 97.4 nmol/L and 17.2 to 72.4 nmol/L, respectively, while the isotopic composition of dissolved Cu ranges from +0.59 to +1.65‰ and +0.48 to +1.20‰, respectively (Table 1). As shown in Figure 3, most of the $\delta^{65}Cu$ values are consistent with previously published data for global rivers (+0.02 to +1.45‰), but are relatively more positive than that of the global discharge-weighted average (+0.68‰) (Vance et al., 2008). The upper reaches (upstream of the TGD), which show increasing $\delta^{65}Cu$ values downstream (Fig. 3), have more positive values of $\delta^{65}Cu$ (+1.01 to +1.45‰) and lower concentrations (16.0-38.9 nmol/L) than the lower reaches (Jiujiang to Nanjing, +0.59 to +1.16‰, 25.3-97.4 nmol/L). The most positive $\delta^{65}Cu$ values are observed in the middle reaches, downstream of the TGD at Guangxingzhou (+1.65‰) and Leigutai (+1.50‰).

Furthermore, a robust correlation ($r = -0.88$, $p < 0.01$, $N = 20$) between Cu concentrations and the $\delta^{65}Cu$ of dissolved Cu in the Yangtze River main channel shows a tendency towards heavier dissolved Cu isotope compositions for lower dissolved Cu concentrations, and the $\delta^{65}Cu$ values of the Yangtze River are always more positive than other rivers with similar Cu concentrations (Fig. 4). In the

following discussion, we review the possible processes that control this Cu-δ^{65}Cu trend.

4. Discussion

4.1. Atmospheric and anthropogenic sources of Cu

Chetelat et al. (2008) estimated that the proportion of cations supplied by atmospheric input to the Yangtze River ranges from 2 to 10%. The maximum measured Cu concentration of atmospheric precipitation from Chongqing to Shanghai is about 315 nmol/L (Ai, 2011; Hu et al., 2012; Liu G. et al., 2014; Peng, 2014). The average annual precipitation of the Yangtze River basin was 1029.6 mm in 2013 and 1100.6 mm in 2014 (data from the Changjiang & Southwest Rivers Water Resources Bulletin). Therefore, the product of average annual precipitation (i.e. 1029.6 mm, 1100.6 mm) and Cu concentration (i.e. 315 nmol/L) can be used to estimate an atmospheric Cu flux over the Yangtze River basin of up to about 21,000 g/km^2/yr. Takano et al. (2014) determined δ^{65}Cu values in rainwater of Japan, finding a range of -0.12 to +0.03‰, and thus presumed the δ^{65}Cu value for atmospheric input to be ~0‰, close to that of the bulk silicate Earth (+0.07 ± 0.10‰ (2SD), Liu et al., 2015; Savage et al., 2015; Moynier et al., 2017). Rain is thus one important pathway delivering Cu (both directly in runoff, and in indirectly via the washing in of solid particles) to the Yangtze River. However, assuming a lithogenic Cu isotope composition, rainwater cannot explain the heavy isotopic compositions observed in the river.

Potential anthropogenic Cu inputs to the river include agriculture (fertilizers, soil

amendments), industrial activities (mining and refinery, fossil fuel combustion, chemical industries) and urban activities (waste incineration, traffic), which are spatially and quantitatively variable (Fekiacova et al., 2015).

Copper is an essential micronutrient required for the growth of animals and plants and is usually added into fertilizer. Long-term application of fertilizer leads to the accumulation of Cu in surface soil (Wei et al., 2007). The leaching of fertilized soils (croplands or farmlands) can transfer fertilizer-derived Cu to rivers (Bengtsson et al., 2006). Phosphorus is the main nutrient element that is widely added to the arable land areas in China. About 8.5×10^6 t P fertilizers were used in 2014, accounting for 14.1% of the total fertilizer (~6.0×10^7 t) used in 2014 (data come from National Bureau of Statistics of China). The draft standard for approval of Cu in the fertilizer is less than 0.0050%, and the measured percent content of Cu in fertilizer ranges from 0.00014 to 0.00022% (Yan et al., 2014). Hence, the Cu/P ratio in the fertilizer ranges from 0.000010 to 0.000016. If we assume that all the dissolved P in the Yangtze River water comes from fertilizer, the dissolved Cu concentration derived from fertilizers can be estimated by using the Cu/P ratio. In so doing, we find that Cu from P fertilizers accounts for less than 0.3% of the Cu concentration in the Yangtze River (see the supplement for details). If we assume a similar Cu content in all (i.e. P and non-P fertilizers), this increases the fertilizer-derived Cu in the river to ~2.1%. Hence, the input of Cu derived from fertilizer is likely small and can be neglected in the analysis of Cu isotopes.

The second possible anthropogenic source of Cu to the Yangtze River is the

industrial processing of ore minerals. There is no significant Cu isotope fractionation during smelting because Cu has a higher boiling point than most smelting temperatures (Gale et al., 1999; Mattielli et al., 2006). Therefore, the δ^{65}Cu of emissions from Cu smelting are likely to reflect the Cu isotope composition of the feedstock (Thapalia et al., 2010). Feedstock deposits are predominantly sulphide minerals (Borrok et al., 2008; Kimball et al., 2009; Mathur et al., 2009), which typically have light Cu isotope compositions and high Cu concentrations (see section 4.3). The Cu concentration of industrial wastewater in China is relatively high, up to 6.4×10^4 nmol/L (Cheng, 2003), while the Cu concentration of mining wastewater in Central South China (located in the Yangtze River basin) is up to 4.6×10^3 nmol/L (Hu et al., 2014), suggesting that mining may have a significant influence on riverine Cu. Evidence for a local industrial source of Cu to the Yangtze River can be seen at Tongling, a famous Cu industrial city located in the lower reaches, where the river has an elevated Cu concentration (97.4 nmol/L) and a less positive δ^{65}Cu value, of +0.61‰ (Table 1).

Urban activities are a third possible anthropogenic source of Cu. Copper is the most abundant trace element measured in brake pads (~6.6%) (McKenzie et al., 2009). Brake pad waste in China contains high Cu concentrations of 10.6% by weight (Zhang et al., 2019). Brake wear from road traffic vehicles is an important source of atmospheric (particulate) Cu concentrations, and can contribute significantly to deposition fluxes of Cu to surface waters (Hulskotte et al., 2007). Dong et al. (2017) found that the Cu concentrations of PM_{10} (particulate matter, diameter ≤10 μm)

collected at a heavily traveled street (Marylebone) were much higher than those from a lightly traveled open urban site (North Kensington) in London, UK (Table 3). About 40% of the total Cu present in the brake wear debris can be leached into solutions by synthetic rainwater after 18 h in batch reactors (Hur et al., 2004). Similarly, about half of the Cu present in PM_{10} can be leached in acetate buffer solution at pH 4.5 (Canepari et al., 2008). To our knowledge, no Cu isotope compositions for Chinese traffic emissions have yet been reported. However, δ^{65}Cu values for European tyres and breaks range from +0.17 to +0.63‰ (Table 3, Dong et al., 2017). By comparison, dissolved Cu isotope compositions close to the huge cities along the Yangtze River, e.g. Chongqing and Wuhan, are characterized by distinctly positive values (+1.04‰, +1.37‰, Table 1), and do not exhibit significantly elevated Cu concentrations (27.3 nmol/L, 25.9 nmol/L, Table 1). Therefore, despite the relatively high Cu concentrations of brake pads, we suggest that urban activities are likely a minor contributor to the distribution of Cu and Cu isotopes in the Yangtze River.

4.2. Lithological control on the enrichment of isotopically heavy dissolved Cu

Bulk silicate Earth has an average δ^{65}Cu of +0.07 ± 0.10‰ (2SD) while different rocks have some measurable differences in δ^{65}Cu (cratonic peridotites: -0.64 to +0.68‰; orogenic peridotites: -0.34 to +1.82‰; basalts: -0.19 to +0.47‰; andesites/dacites: +0.04 to +0.38‰) (Liu et al., 2015; Savage et al., 2015; Moynier et al., 2017). Weathering can also drive isotopic fractionation (e.g. Mathur et al., 2012; Vance et al., 2016). The lithological distribution and the weathering of rocks in the drainage basin may therefore influence riverine dissolved Cu isotope compositions.

Carbonates are characterized by relatively high Ca/Na and Mg/Na ratios, while silicates and evaporites have lower ratios (Gaillardet et al., 1999; Dessert et al., 2003). The Na-normalized ratios (Mg/Na vs. Ca/Na, Fig. S1 in supplement) for the Yangtze River water samples indicate that carbonates and silicates control the dissolved concentrations of major cations. Typically, carbonates and/or evaporites have high concentrations of Sr and low $^{87}Sr/^{86}Sr$ ratios, while silicates have low concentrations and high $^{87}Sr/^{86}Sr$ ratios (Palmer and Edmond, 1989; Palmer and Edmond, 1992). A plot of $^{87}Sr/^{86}Sr$ versus 1/Sr (Fig. S2 in supplement) shows that the Yangtze River mainstream water chemistry is mainly dominated by the contribution of carbonate weathering. Decreasing concentrations of Ca and Mg from the upper to lower reaches (Fig. 2) suggest a gradually increasing contribution of silicate rocks in the middle-lower reaches.

Dissolved Cu/Ca ratios (μmol/mol) decline from ~30 to ~15 in the upper reaches, then increase markedly in the middle-lower reaches to a maximum of ~100 (Fig. 5). These changes are consistent with changing Cu/Ca ratios of the major source rocks. Silicate rocks have an average Cu concentration of 28 μg/g and CaO percentage of 3.59% (Rudnick and Gao, 2003), leading to a high Cu/Ca ratio of ~690 μmol/mol. The extensive Cu sulphide deposits present close to the lower reaches of the Yangtze River (see section 4.3) will also exhibit very elevated Cu/Ca ratios. By contrast, carbonate rocks have an average Cu concentration of 14 ± 9 μg/g (Graf, 1960). For limestone, with 95-100% $CaCO_3$, carbonate Cu/Ca will range from ~8 to ~40 μmol/mol, while for pure dolomite ($CaMg(CO_3)_2$) it will range from ~15 to ~70

μmol/mol. Thus, the increasing Cu/Ca ratios in the lower reaches are consistent with an increasing contribution of solutes from the weathering of silicates or Cu sulphide deposits with high Cu/Ca ratios.

Dissolved Cu isotope compositions exhibit the reverse trend to Cu/Ca, becoming isotopically heavier downstream in the upper and middle reaches, and then isotopically lighter in and lower reaches (Fig. 3). In fact, most data from the main stream of the Yangtze fall close to a mixing line in 1/Cu vs. δ^{65}Cu space (Fig. 6), suggesting that dissolved Cu and Cu isotope compositions could reflect mixing of two sources: (1) a low Cu concentration, high δ^{65}Cu end-member (at about +1.6‰) from the upper reaches and (2) a higher Cu concentration, lower δ^{65}Cu end-member (at about +0.6‰) in the lower reaches (Fig. 6).

Clastic silicate rocks exhibit Cu isotope compositions of +0.08 ± 0.20‰ (2SD, Moynier et al., 2017). However, a range of soils developed on silicate (granitoid and basaltic) rock substrates exhibit the preferential loss of isotopically heavy Cu during oxic weathering, suggested to reflect partitioning between aqueous organic complexes and/or incorporation in Fe (hydr)-oxides retained in the soil (Vance et al., 2016; Little et al., 2019). Oxidative weathering of sulphides is also expected to mobilise isotopically heavy Cu (e.g., Kimball et al., 2009; Mathur et al., 2005, 2012), discussed in detail in section 4.3. Therefore, weathering of silicates and/or sulphides is a plausible driver of heavy Cu isotope compositions (compared to the solid Earth, at about ~0‰) in the dissolved pool of the Yangtze River.

The upper reaches of the Yangtze are primarily under the influence of carbonate

weathering, providing one possible origin of the high δ^{65}Cu end-member. At present, little is known about the Cu isotope composition of carbonate rocks, or any potential isotopic fractionation during carbonate weathering. In ore bodies, Cu carbonate minerals are isotopically heavy compared to coexisting Cu sulphides (e.g. Asael et al., 2007), consistent with predictions from ab initio calculations (e.g., Fujii et al., 2013). However, we consider it unlikely that the unusually heavy Cu isotope compositions observed in the upper-middle reaches of the Yangtze (up to +1.65‰) reflect a carbonate Cu source. We return to discuss the origin of these high δ^{65}Cu values in section 4.4.

Rather than mixing between two end-members with different Cu-δ^{65}Cu characteristics, the evolution of dissolved δ^{65}Cu values in the Yangtze River could instead result from variability in the trapping efficiency of isotopically light Cu in soils across the basin. The greater the trapping efficiency, the lower the riverine dissolved Cu concentration and heavier its isotopic composition, which would lead to a negative correlation between Cu concentrations and δ^{65}Cu values (Fig. 4). For example, from Chongqing to Yichang, the Cu concentration decreases (Fig. S3 in supplement) (as the water discharge increases by ~30%); this decrease is associated with an accumulation of isotopically heavy Cu in the middle reaches (Fig. 3). However, this hypothesis is speculative; testing it would require a means to estimate the trapping efficiency of Cu in soils across the basin.

4.3. Copper isotope fractionation during weathering of ore deposits

Markedly elevated dissolved Cu concentrations (69 to 97 nmol/L) and less positive δ^{65}Cu values (+0.59 to +0.63‰) are observed in the lower reaches of the Yangtze River, from Jiujiang to Tongling (Figs. 3, S3). We suggest that these values reflect leaching of the extensive Cu sulphide-rich deposits located near the mainstream of Yangtze River in this region (Fig. 7). These deposits have variably light Cu isotope compositions (-2.10 to +0.17‰, Ouyang et al., 2017; -0.54 to +0.95‰, Wang et al., 2014) (Fig. 3), but the oxidative weathering of sulphide-rich rocks is thought to lead to the mobilization of isotopically heavy Cu (Kimball et al., 2009; Mathur et al., 2005, 2012; Mathur and Fantle, 2015; Lv et al., 2016). Surface water and groundwater samples in the Tongling area have wide-ranging δ^{65}Cu values (-0.13 to +6.90‰), generally heavier than the primary ore materials (chalcopyrite: -0.04 ± 0.26‰ (n = 9); pyrite: +0.61 ± 0.94‰ (n = 4), Su et al., 2018). Dissolved Cu isotope compositions of +0.59‰ to +0.63‰ from Jiujiang to Tongling in the Yangtze main stream, and of +0.48‰ for the Hongxing River tributary (TLHX-1), are close to those of mine leachates from the Tongling ore fields (+0.30‰, Su et al., 2018), suggesting that this section of the Yangtze is significantly influenced by Cu that originated from mining.

4.4. Fractionation of Cu isotopes in the river channel

The construction of the TGD led to sedimentation of particulate material and an increase in the transparency and dissolved oxygen content of the water column in the TGR (Huang, 2008). As a result, phytoplankton, consisting of Cyanophyta, Baeillariophyta and Chiorophyta, increase in abundance from Chongqing to Yichang.

407 Total biomass increases from 0.0019 mg/L to 0.0040 mg/L (Huang, 2008). Cellular
408 Cu uptake by phytoplankton favours incorporation of light Cu isotopes (e.g. Navarette
409 et al., 2011), and could thus lead to the enrichment of isotopically heavy Cu in the
410 dissolved phase. However, assuming a mean cellular Cu:C ratio of 4.1 μmol/mol for
411 phytoplankton (Sunda and Huntsman, 1995), we estimate that less than 0.01%
412 dissolved Cu is incorporated into phytoplankton cells in the TGR, with a resultant
413 negligible influence of biological uptake on the fractionation of Cu isotopes.

414 The free Cu^{2+} ion occurs primarily as an aquacomplex in inorganic freshwater
415 solutions, as $Cu(H_2O)_5^{2+}$ (Sherman, 2001). However, many previous studies have
416 concluded that dissolved Cu in rivers and oceans is very strongly bound to organic
417 ligands (e.g., Skrabal et al., 1997; Wells et al., 1998; Shank et al., 2004; Moffett and
418 Dupont, 2007), with less than 1% of the total dissolved fraction present as free Cu^{2+}
419 (Moffett and Dupont, 2007; Thompson et al., 2014). This organic complexation may
420 lead to isotopically heavy Cu in the dissolved phase because of the preferential
421 complexation of heavy Cu isotopes by organic ligands (Schauble, 2004; Vance et al.,
422 2008; Bigalke et al., 2011; Ryan et al., 2014). Experimental estimates of
423 $\Delta^{65}Cu_{complex\text{-}free}$ vary with ligand-binding strength, from +0.14 to +0.84‰ (Ryan et al.,
424 2014).

425 While organic complexation retains isotopically heavy Cu in the dissolved phase,
426 scavenging may remove isotopically light Cu to the particulate phase (e.g., Takano et
427 al., 2014). For example, sorption of Cu to kaolinite favours light Cu isotopes, with
428 experimental estimates of $\Delta^{65}Cu_{sorbed\text{-}free}$ = -0.2 to -0.8‰ at low ionic strength (Li et

429 al., 2015). As discussed, the construction of the TGD caused a significant amount of
430 sediment deposition in the Three Gorges Reservoir (TGR, from Chongqing to
431 Yichang), as well as a decrease in the concentration of suspended particulate material
432 in the river from ~1000 mg/L to ~100 mg/L in July 2003, 2005 and 2007 (Huang,
433 2008; Ding et al., 2013). Copper concentrations in sediments of the TGR range from
434 36.5 to 93.9 μg/g (Bing et al., 2016), almost all of which are enriched compared to the
435 detrital background Cu concentration of 35 μg/g (Zhao et al., 2017). The sediments,
436 which consist of numerous clay minerals and organic/inorganic colloids, are likely to
437 be enriched in Cu by adsorption.

438 Consistent with the hypothesised scavenging removal of isotopically light Cu on
439 particles, dissolved δ^{65}Cu values increase and Cu concentations decrease downstream
440 towards the TGD (Fig. 3, Fig. S3). Furthermore, sorption of cations on negatively
441 charged mineral surfaces is more energetically favourable at higher pH; we observe a
442 positive correlation ($r = 0.78$, $p < 0.01$, $N = 10$) between dissolved Cu isotope
443 compositions and pH in the upper reaches (Fig. 8), consistent with increased
444 adsorption of light Cu onto clay particles.

445 The most positive δ^{65}Cu values (up to +1.65‰) are observed in the middle
446 reaches downstream of the TGD, from Yichang to Chibi (Fig. 3). To our knowledge,
447 Cu isotope compositions in this section of the Yangtze are the heaviest yet reported in
448 any river system worldwide. We suggest that these values reflect the continued impact
449 of the TGD downstream. Notably, δ^{65}Cu values increase in concert with dissolved
450 oxygen, both upstream and downstream of the TGD (Fig. S4). This relationship

suggests an impact on Cu isotope geochemistry of enhanced productivity, via the enhanced production of strong organic ligands, and/or the presence of particulate phases (e.g., Fe-Mn oxides, clays), which continue to scavenge isotopically light Cu (e.g., Little et al., 2014; Li et al., 2015; Ijichi et al., 2018). More detailed evaluation of these possibilities requires an analysis of particulate phase Cu isotope compositions.

Though we cannot isolate the individual roles of organic complexation and scavenging, their combined impact on aqueous Cu isotope compositions can be modelled following Vance et al. (2008), by assuming equilibrium partitioning between the dissolved and particulate phase, illustrated in Figure 9. For a starting Cu pool with the maximum measured Cu concentration (~100 nmol/L) and minimum dissolved δ^{65}Cu value (at +0.6‰), the best fit $\Delta^{65}Cu_{diss\text{-}part}$ is about +1‰. However, this model (dashed curve, Fig. 9) does not provide a good fit to the dataset, particularly at intermediate Cu concentrations. If we assume that the samples from the lower reaches (with high Cu concentrations and less positive δ^{65}Cu values) record the impact of Cu supply from the weathering of Cu sulphide deposits (section 4.3), and instead set the initial Cu concentration and δ^{65}Cu at 40 nmol/L and +1‰, the best fit $\Delta^{65}Cu_{diss\text{-}part}$ is about +0.8‰. This alternative model (solid line, Fig. 9) provides a significantly improved fit to the data from the upper and middle reaches of the Yangtze mainstream. A fractionation factor of +0.8‰ is also broadly consistent with experimental constraints on organic complexation and sorption to particulates, and with the observed offset between the two phases in a small natural river system (the Itchen, UK; Vance et al., 2008).

To conclude, we suggest that sedimentation and scavenging of Cu driven by the intercept of the TGD has a significant impact on the Cu isotope geochemistry of the Yangtze River, and is likely responsible for the globally anomalous heavy Cu isotope compositions observed in its upper and middle reaches. Future work should test this hypothesis by coupling particulate and dissolved phase Cu isotope ratio analysis.

Finally, we note that the most downstream site (NJ-1, Nanjing) also has more positive δ^{65}Cu than the three upstream sites influenced by Cu sulphide-rich ore deposits. About 75% of Cu is lost between these upstream sites and NJ-1, suggesting that strong adsorption of Cu onto particles occurs at this location due to the tidal influence that enhances the concentration of suspended particulate matter.

5. Conclusions

This study presents dissolved Cu isotope compositions and Cu concentrations for the main channel of the Yangtze River and its several tributaries. The Yangtze River exhibits more positive δ^{65}Cu values (range: +0.59 to +1.65‰) than other rivers at similar Cu concentrations, and there is a tendency towards heavier dissolved Cu isotope compositions at lower Cu concentrations.

Isotopically heavy Cu in global rivers (compared to lithogenic Cu, at about 0‰) is believed to reflect a) oxidative weathering, which mobilises isotopically heavy Cu, and b) partitioning in the river between an isotopically heavy, organically complexed dissolved pool, and an isotopically light pool, sorbed to particulates. While these processes are undoubtedly important in the Yangtze River, they do not explain its apparently anomalous Cu isotope geochemistry compared to other rivers.

We find two key features of the Yangtze River basin that contribute to the unique Cu isotope geochemistry of the river. First, we suggest that the Three Gorges Dam (TGD) has had a major impact on the Cu isotope geochemistry of the upper and middle reaches. Second, we suggest that weathering of extensive Cu sulphide deposits between Jiujiang and Tongling dominates the geochemistry of the lower reaches.

In the upper reaches, upstream of the TGD, we observe increasing δ^{65}Cu values and decreasing Cu concentrations associated with increasing pH. The construction of TGD has led to extensive sedimentation, and we suggest that the sorptive removal of isotopically light Cu onto particles explains the observed trend towards isotopically heavy Cu in the dissolved phase. Downstream of the TGD, in the middle reaches, δ^{65}Cu values increase to a maximum of +1.65‰. We suggest that this trend reflects the downstream influence of the TGD, which is associated with increasing dissolved oxygen levels that may drive elevated primary productivity.

In the lower reaches, oxidative weathering of isotopically light Cu sulphide-rich deposits leads to elevated Cu concentrations and lighter Cu isotope compositions in the river. The overall relationship between dissolved Cu and δ^{65}Cu in the Yangtze mainstream thus reflects mixing between these high concentration, low δ^{65}Cu, Cu sulphide-influenced waters, and the lower concentration, higher δ^{65}Cu waters from upstream.

Acknowledgments

We are grateful for the thoughtful comments of Damien Guinoiseau and four anonymous reviewers, which significantly improved three earlier versions of this

manuscript. This work has been supported financially by the National Key Research and Development Project of China (2016YFC0600309) and National Natural Science Foundation of China (Nos. 41473007, 41673013), the Yangtze Estuary Marine Scientific Expedition Voyage of the NSFC (voyage ID: NORC2015-03; NORC2017-03). SHL acknowledges support from NERC (NE/P018181/1). We are also thankful to the help of Jincun Liu, Meilian Zhou, Zhifang Hu, Dong Han and Yong Wang for their field work.

References

Ai, D., 2011. Chemical characteristics of wet precipitation in Shanghai and its source analysis. East China Normal University. (in Chinese with English abstract)

Asael, D., Matthews, A., Bar-Matthews, M., Halicz, L., 2007. Copper isotope fractionation in sedimentary copper mineralization (Timna Valley, Israel). Chem. Geol. 243(3–4), 238-254.

Baconnais, I., Rouxel, O., Dulaquais, G., Boye, M., 2019. Determination of the copper isotope composition of seawater revisited: A case study from the Mediterranean Sea. Chem. Geol. 511, 465-480.

Balcaen, L., Schrijver, I.D., Moens, L., Vanhaecke, F., 2005. Determination of the $^{87}Sr/^{86}Sr$ isotope ratio in USGS silicate reference materials by multi-collector ICP–mass spectrometry. Int. J. Mass Spectrom. 242(2), 251-255.

Balistrieri, L.S., Borrok, D.M., Wanty, R.B., Ridley, W.I., 2008. Fractionation of Cu and Zn isotopes during adsorption onto amorphous Fe(III) oxyhydroxide: Experimental mixing of acid rock drainage and ambient river water. Geochim.

Cosmochim. Acta 72(2), 311-328.

Bengtsson, H., Alvenäs, G., Nilsson, S.I., Hultman, B., Öborn, I., 2006. Cadmium, copper and zinc leaching and surface run-off losses at the Öjebyn farm in Northern Sweden—Temporal and spatial variation. Agric. Ecosyst. Environ. 113(1), 120-138.

Bermin, J., Vance, D., Archer, C., Statham, P.J., 2006. The determination of the isotopic composition of Cu and Zn in seawater. Chem. Geol. 226(3), 280-297.

Bigalke, M., Weyer, S., Wilcke, W., 2011. Stable Cu isotope fractionation in soils during oxic weathering and podzolization. Geochim. Cosmochim. Acta 75(11), 3119-3134.

Bing, H.J., Zhou, J., Wu, Y.H., Wang, X.X., Sun, H.Y., Li, R., 2016. Current state, sources, and potential risk of heavy metals in sediments of Three Gorges Reservoir, China. Environ. Pollut. 214, 485-496.

Borrok, D.M., Nimick, D.A., Wanty, R.B., Ian Ridley, W., 2008. Isotopic variations of dissolved copper and zinc in stream waters affected by historical mining. Geochim. Cosmochim. Acta 72(2), 329-344.

Bouchez, J., Lajeunesse, E., Gaillardet, J., France-Lanord, C., Dutra-Maia, P., Maurice, L., 2010. Turbulent mixing in the Amazon River: The isotopic memory of confluences. Earth. Planet. Sci. Lett. 290(1-2), 37-43.

Canepari, S., Perrino, C., Olivieri, F., Astolfi, M.L., 2008. Characterisation of the traffic sources of PM through size-segregated sampling, sequential leaching and ICP analysis. Atmos. Environ. 42(35), 8161-8175.

Chen, J., Wang, F., Xia, X., Zhang, L., 2002. Major element chemistry of the Changjiang (Yangtze River). Chem. Geol. 187(3), 231-255.

Chen, X., Yan, Y., Fu, R., Dou, X., Zhang, E., 2008. Sediment transport from the Yangtze River, China, into the sea over the Post-Three Gorge Dam Period: A discussion. Quatern. Int. 186(1), 55-64.

Chen, X., Zong, Y., Zhang, E., Xu, J., Li, S., 2001. Human impacts on the Changjiang (Yangtze) River basin, China, with special reference to the impacts on the dry season water discharges into the sea. Geomorphology 41(2), 111-123.

Chen, Z., Li, J., Shen, H., Wang, Z., 2001. Yangtze River of China: historical analysis of discharge variability and sediment flux. Geomorphology 41(2), 77-91.

Cheng, S., 2003. Heavy metal pollution in China: origin, pattern and control. Environ. Sci. Pollut. Res. 10(3), 192-198.

Chetelat, B., Liu, C.Q., Gaillardet, J., Wang, Q.L., Zhao, Z.Q., Liang, C.S., Xiao, Y.K., 2009. Boron isotopes geochemistry of the Changjiang basin rivers. Geochim. Cosmochim. Acta 73(20), 6084-6097.

Chetelat, B., Liu, C.Q., Wang, Q., Zhang, G., 2013. Assessing the influence of lithology on weathering indices of Changjiang river sediments. Chem. Geol. 359, 108-115.

Chetelat, B., Liu, C.Q., Zhao, Z.Q., Wang, Q.L., Li, S.L., Li, J., Wang, B.L., 2008. Geochemistry of the dissolved load of the Changjiang Basin rivers: anthropogenic impacts and chemical weathering. Geochim. Cosmochim. Acta 72(17), 4254-4277.

Dessert, C., Dupré, B., Gaillardet, J., François, L.M., Allègre, C.J., 2003. Basalt weathering laws and the impact of basalt weathering on the global carbon cycle. Chem. Geol. 202(3–4), 257-273.

Ding, T., Gao, J., Shi, G., Chen, F., Wang, C., Han, D., Luo, X., 2013. The contents and mineral and chemical compositions of suspended particulate materials in the Yangtze River, and their geological and environmental implications. Acta Geologica Sinica 87(5), 634-660. (in Chinese with English abstract)

Ding, T., Gao, J., Tian, S., Shi, G., Chen, F., Wang, C., Luo, X., Han, D., 2014. Chemical and Isotopic Characteristics of the Water and Suspended Particulate Materials in the Yangtze River and Their Geological and Environmental Implications. Acta Geologica Sinica -English Edition 88(1), 276-360.

Ding, T., Wan, D., Wang, C., Zhang, F., 2004. Silicon isotope compositions of dissolved silicon and suspended matter in the Yangtze River, China. Geochim. Cosmochim. Acta 68(2), 205-216.

Dong, S., Gonzalez, R.O., Harrison, R.M., Green, D., North, R., Fowler, G., Weiss, D., 2017. Isotopic signatures suggest important contributions from recycled gasoline, road dust and non-exhaust traffic sources for copper, zinc and lead in PM10 in London, United Kingdom. Atmos. Environ. 165, 88-98.

Du, Y., Cai, S., Zhang, X., Zhao, Y., 2001. Interpretation of the environmental change of Dongting Lake, middle reach of Yangtze River, China, by 210 Pb measurement and satellite image analysis. Geomorphology 41(2), 171-181.

Ehrlich, S., Butler, I., Halicz, L., Rickard, D., Oldroyd, A., Matthews, A., 2004.

Experimental study of the copper isotope fractionation between aqueous Cu(II) and covellite, CuS. Chem. Geol. 209(3–4), 259-269.

Fekiacova, Z., Cornu, S., Pichat, S., 2015. Tracing contamination sources in soils with Cu and Zn isotopic ratios. Sci. Total Environ. 517, 96-105.

Fernandez, A., Borrok, D.M., 2009. Fractionation of Cu, Fe, and Zn isotopes during the oxidative weathering of sulfide-rich rocks. Chem. Geol. 264(1), 1-12.

Fujii, T., Moynier, F., Abe, M., Nemoto, K., Albarède, F., 2013. Copper isotope fractionation between aqueous compounds relevant to low temperature geochemistry and biology. Geochim. Cosmochim. Acta 110(3), 29-44.

Fujii, T., Moynier, F., Blichert-Toft, J., Albarède, F., 2014. Density functional theory estimation of isotope fractionation of Fe, Ni, Cu, and Zn among species relevant to geochemical and biological environments. Geochim. Cosmochim. Acta 140, 553-576.

Gaillardet, J., Dupré, B., Louvat, P., Allègre, C.J., 1999. Global silicate weathering and CO_2 consumption rates deduced from the chemistry of large rivers. Chem. Geol. 159(1–4), 3-30.

Gale, N. H., Woodhead, A. P., Stos-Gale, Z. A., Walder, A., Bowen, I., 1999. Natural variations detected in the isotopic composition of copper: possible applications to archaeology and geochemistry. Int. J. Mass Spectrom. 184(1), 1-9.

Gao, S., Luo, T., Zhang, B., Zhang, H., Han, Y., Zhao, Z., Hu, Y., 1998. Chemical composition of the continental crust as revealed by studies in East China. Geochim. Cosmochim. Acta 62(11), 1959-1975.

Graf, D.L., 1960. Geochemistry of carbonate sediments and sedimentary carbonate rocks: pt. III, Minor element distribution. Circular no. 301. pp, 71.

Guinoiseau, D., Bouchez, J., Gélabert, A., Louvat, P., Filizola, N., Benedetti, M.F., 2016. The geochemical filter of large river confluences. Chem. Geol. 441, 191-203.

Guinoiseau, D., Bouchez, J., Gélabert, A., Louvat, P., Moreira-Turcq, P., Filizola, N., Benedetti, M.F., 2018. Fate of particulate copper and zinc isotopes at the Solimões-Negro river confluence, Amazon Basin, Brazil. Chem. Geol. 489, 1-15.

Guinoiseau, D., Gélabert, A., Allard, T., Louvat, P., Moreira-Turcq, P., Benedetti, M. F., 2017. Zinc and copper behaviour at the soil-river interface: New insights by Zn and Cu isotopes in the organic-rich Rio Negro basin. Geochim. Cosmochim. Acta 213, 178-197.

Guo, H., Hu, Q., Zhang, Q., Feng, S., 2012. Effects of the three gorges dam on Yangtze river flow and river interaction with Poyang Lake, China: 2003–2008. J. Hydrol. 416, 19-27.

Hans, U., Kleine, T., Bourdon, B., 2013. Rb-Sr chronology of volatile depletion in differentiated protoplanets: BABI, ADOR, and ALL revisited. Earth. Planet. Sci. Lett. 374(4), 204-214.

Hou, Q., Zhou, L., Gao, S., Zhang, T., Feng, L., Yang, L., 2016. Use of Ga for mass bias correction for the accurate determination of copper isotope ratio in the NIST SRM 3114 Cu standard and geological samples by MC-ICPMS. J. Anal.

At. Spectrom. 31(1), 280-287.

Hu, C., Ke, L., Tong, L., Zhou, W., 2012. Characteristics and source analysis of heavy metals in atmospheric precipitation. Environmental Pollution & Control, 34(12), 26-30. (in Chinese with English abstract)

Hu, X.F., Jiang, Y., Shu, Y., Hu, X., Liu, L., Luo, F., 2014. Effects of mining wastewater discharges on heavy metal pollution and soil enzyme activity of the paddy fields. J. Geochem. Explor. 147, 139-150.

Huang, H., 2008. A study on the effects of sediment deposition to the plankton of the three gorges reservoir. Southwest University. (in Chinese with English abstract)

Hulskotte, J., Denier van der Gon, H., Visschedijk, A., Schaap, M., 2007. Brake wear from vehicles as an important source of diffuse copper pollution. Water Sci. Technol. 56(1), 223-231.

Hur, J., Schlautman, M.A., Yim, S., 2004. Effects of organic ligands and pH on the leaching of copper from brake wear debris in model environmental solutions. J. Environ. Monit. 6(1), 89-94.

Ijichi, Y., Ohno, T., Sakata, S., 2018. Copper isotopic fractionation during adsorption on manganese oxide: Effects of pH and desorption. Geochem. J. 52(2), e1-e6.

Kimball, B.E., Mathur, R., Dohnalkova, A.C., Wall, A.J., Runkel, R.L., Brantley, S.L., 2009. Copper isotope fractionation in acid mine drainage. Geochim. Cosmochim. Acta 73(5), 1247-1263.

Kusonwiriyawong, C., Bigalke, M., Abgottspon, F., Lazarov, M., Schuth, S., Weyer,

S., Wilcke, W., 2017. Isotopic variation of dissolved and colloidal iron and copper in a carbonatic floodplain soil after experimental flooding. Chem. Geol. 459, 13-23.

Larson, P.B., Maher, K., Ramos, F.C., Chang, Z., Gaspar, M., Meinert, L.D., 2003. Copper isotope ratios in magmatic and hydrothermal ore-forming environments. Chem. Geol. 201(3–4), 337-350.

Li, D., Liu, S.A., Li, S., 2015. Copper isotope fractionation during adsorption onto kaolinite: Experimental approach and applications. Chem. Geol. 396, 74-82.

Li, Q., Yu, M., Lu, G., Cai, T., Bai, X., Xia, Z., 2011. Impacts of the Gezhouba and Three Gorges reservoirs on the sediment regime in the Yangtze River, China. J. Hydrol. 403(3), 224-233.

Little, S.H., Archer, C., Milne, A., Schlosser, C., Achterberg, E.P., Lohan, M.C., Vance, D., 2018. Paired dissolved and particulate phase Cu isotope distributions in the South Atlantic. Chem. Geol. 502, 29-43.

Little, S.H., Munson, S., Prytulak, J., Coles, B.J., Hammond, S.J., Widdowson, M., 2019. Cu and Zn isotope fractionation during extreme chemical weathering. Geochim. Cosmochim. Acta 263, 85-107.

Little, S.H., Vance, D., Walker-Brown, C., Landing, W.M., 2014. The oceanic mass balance of copper and zinc isotopes, investigated by analysis of their inputs, and outputs to ferromanganese oxide sediments. Geochim. Cosmochim. Acta 125, 673-693.

Liu, G., Shi, Z., Zeng, J., Su, W., Yang, F., Dong, A., 2014. Summary of

characteristics of heavy metals in atmospheric precipitation. Environmental Science and Management, 39(11), 41-44. (in Chinese with English abstract)

Liu, S.A., Huang, J., Liu, J., Wörner, G., Yang, W., Tang, Y.J., Chen, Y., Tang, L., Zheng, J., Li, S., 2015. Copper isotopic composition of the silicate Earth. Earth Planet. Sci. Lett. 427, 95-103.

Liu, S.A., Li, D., Li, S., Teng, F.Z., Ke, S., He, Y., Lu, Y., 2014. High-precision copper and iron isotope analysis of igneous rock standards by MC-ICP-MS. J. Anal. At. Spectrom. 29(1), 122-133.

Luo, X., Yang, S., Zhang, J., 2012. The impact of the Three Gorges Dam on the downstream distribution and texture of sediments along the middle and lower Yangtze River (Changjiang) and its estuary, and subsequent sediment dispersal in the East China Sea. Geomorphology 179, 126-140.

Lv, Y., Liu, S.A., Zhu, J.M., Li, S., 2016. Copper and zinc isotope fractionation during deposition and weathering of highly metalliferous black shales in central China. Chem. Geol. 445, 24-35.

Maréchal, C.N., Télouk, P., Albarède, F., 1999. Precise analysis of copper and zinc isotopic compositions by plasma-source mass spectrometry. Chem. Geol. 156(1–4), 251-273.

Mathur, R., Fantle, M. S., 2015. Copper isotopic perspectives on supergene processes: implications for the global Cu cycle. Elements 11(5), 323-329.

Mathur, R., Jin, L., Prush, V., Paul, J., Ebersole, C., Fornadel, A., Williams, J.Z., Brantley, S., 2012. Cu isotopes and concentrations during weathering of black

shale of the Marcellus Formation, Huntingdon County, Pennsylvania (USA). Chem. Geol. 304, 175-184.

Mathur, R., Munk, L.A., Townley, B., Gou, K.Y., Gómez Miguélez, N., Titley, S., Chen, G.G., Song, S., Reich, M., Tornos, F., Ruiz, J., 2014. Tracing low-temperature aqueous metal migration in mineralized watersheds with Cu isotope fractionation. Appl. Geochem. 51, 109-115.

Mathur, R., Ruiz, J., Titley, S., Liermann, L., Buss, H., Brantley, S., 2005. Cu isotopic fractionation in the supergene environment with and without bacteria. Geochim. Cosmochim. Acta 69(22), 5233-5246.

Mathur, R., Titley, S., Barra, F., Brantley, S., Wilson, M., Phillips, A., Munizaga, F., Maksaev, V., Vervoort, J., Hart, G., 2009. Exploration potential of Cu isotope fractionation in porphyry copper deposits. J. Geochem. Explor. 102(1), 1-6.

Mattielli, N., Rimetz, J., Petit, J., Perdrix, E., Deboudt, K., Flament, P., Weis, D., 2006. Zn-Cu isotopic study and speciation of airborne metal particles within a 5-km zone of a lead/zinc smelter. Goldschmidt Conference Abstracts, A401.

McKenzie, E.R., Money, J.E., Green, P.G., Young, T.M., 2009. Metals associated with stormwater-relevant brake and tire samples. Sci. Total Environ. 407(22), 5855-5860.

Moffett, J.W., Dupont, C., 2007. Cu complexation by organic ligands in the sub-arctic NW Pacific and Bering Sea. Deep Sea Res. Part 1 Oceanogr. Res. Pap. 54(4), 586-595.

Moynier, F., Vance, D., Fujii, T., Savage, P., 2017. The Isotope Geochemistry of Zinc

and Copper. Rev. Mineral. Geochem. 82(1), 543-600.

Navarrete, J.U., Borrok, D.M., Viveros, M., Ellzey, J.T., 2011. Copper isotope fractionation during surface adsorption and intracellular incorporation by bacteria. Geochim. Cosmochim. Acta 75(3), 784-799.

Ouyang, X., Di, Y., Wang, C., Zhang, D., Yang, Q., Wu, B., Wang, Q., Luo, Z., 2017. Genesis of Dongxiang copper deposit in Jiangxi Province: Constraints from copper and sulfur isotopes. Mineral Deposits, 36(1), 250-264. (in Chinese with English abstract)

Palmer, M.R., Edmond, J.M., 1989. The strontium isotope budget of the modern ocean. Earth Planet. Sci. Lett. 92(1), 11-26.

Palmer, M.R., Edmond, J.M., 1992. Controls over the strontium isotope composition of river water. Geochim. Cosmochim. Acta 56(5), 2099-2111.

Peng, Y., 2014. Concentrations and Deposition Fluxes of Heavy Metals in Precipitation in Core Urban Areas, Chongqing. Southwest University. (in Chinese with English abstract)

Pokrovsky, O., Viers, J., Emnova, E., Kompantseva, E., Freydier, R., 2008. Copper isotope fractionation during its interaction with soil and aquatic microorganisms and metal oxy (hydr) oxides: possible structural control. Geochim. Cosmochim. Acta 72(7), 1742-1757.

Rudnick, R.L., Gao, S., 2003. Composition of the continental crust. The crust, treatise on geochemistry, Amsterdam 3, 1-64.

Ryan, B.M., Kirby, J.K., DeGryse, F., Scheiderich, K., McLaughlin, M.J., 2014.

Copper isotope fractionation during equilibration with natural and synthetic ligands. Environ. Sci. Techno. 48(15), 8620-8626.

Savage, P.S., Moynier, F., Chen, H., Shofner, G., Siebert, J., Badro, J., Puchtel, I.S., 2015. Copper isotope evidence for large-scale sulphide fractionation during Earth's differentiation. Geochem. Perspect. Lett. 1, 53-64.

Schauble, E.A., 2004. Applying Stable Isotope Fractionation Theory to New Systems. Rev. Mineral. Geochem. 55(1), 65-111.

Shank, G.C., Skrabal, S.A., Whitehead, R.F., Avery, G.B., Kieber, R.J., 2004. River discharge of strong Cu-complexing ligands to South Atlantic Bight waters. Mar. Chem. 88(1–2), 41-51.

Sherman, M., D., 2001. Quantum chemistry and classical simulations of metal complexes in aqueous solutions. Rev. Mineral. Geochem. 42(1), 273-317.

Sherman, D.M., 2013. Equilibrium isotopic fractionation of copper during oxidation/reduction, aqueous complexation and ore-forming processes: Predictions from hybrid density functional theory. Geochim. Cosmochim. Acta 118(10), 85–97.

Skrabal, S.A., Donat, J.R., Burdige, D.J., 1997. Fluxes of copper- complexing ligands from estuarine sediments. Limnol. Oceanogr. 42(5), 992-996.

Song, S., Mathur, R., Ruiz, J., Chen, D., Allin, N., Guo, K., Kang, W., 2016. Fingerprinting two metal contaminants in streams with Cu isotopes near the Dexing Mine, China. Sci. Total Environ. 544, 677-685.

Su, J., Mathur, R., Brumm, G., D'amico, P., Godfrey, L., Ruiz, J., Song, S., 2018.

Tracing Copper Migration in the Tongling Area through Copper Isotope Values in Soils and Waters. Inter. J. Env. Res. Pub. Heal. 15(12), 2661.

Sunda, W.G., Huntsman, S.A., 1995. Regulation of copper concentration in the oceanic nutricline by phytoplankton uptake and regeneration cycles. Limnol. Oceanogr. 40(1), 132-137.

Takano, S., Tanimizu, M., Hirata, T., Sohrin, Y., 2014. Isotopic constraints on biogeochemical cycling of copper in the ocean. Nat. Commun. 5, 5663.

Thapalia, A., Borrok, D.M., Van Metre, P.C., Musgrove, M.L., Landa, E.R., 2010. Zn and Cu isotopes as tracers of anthropogenic contamination in a sediment core from an urban lake. Environ. Sci. Technol. 44(5), 1544-1550.

Thompson, C.M., Ellwood, M.J., 2014. Dissolved copper isotope biogeochemistry in the Tasman Sea, SW Pacific Ocean. Mar. Chem. 165, 1-9.

Thompson, C.M., Ellwood, M.J., Sander, S.G., 2014. Dissolved copper speciation in the Tasman Sea, SW Pacific Ocean. Mar. Chem. 164(5), 84-94.

Vance, D., Archer, C., Bermin, J., Perkins, J., Statham, P.J., Lohan, M.C., Ellwood, M.J., Mills, R.A., 2008. The copper isotope geochemistry of rivers and the oceans. Earth Planet. Sci. Lett. 274(1), 204-213.

Vance, D., Matthews, A., Keech, A., Archer, C., Hudson, G., Pett-Ridge, J., Chadwick, O.A., 2016. The behaviour of Cu and Zn isotopes during soil development: Controls on the dissolved load of rivers. Chem. Geol. 445, 36-53.

Wall, A.J., Mathur, R., Post, J.E., Heaney, P.J., 2011. Cu isotope fractionation during bornite dissolution: An in situ X-ray diffraction analysis. Ore Geol. Rev. 42(1),

62-70.

Wang, Q.L., Chetelat, B., Zhao, Z.Q., Ding, H., Li, S.L., Wang, B.L., Li, J., Liu, X.L., 2015. Behavior of lithium isotopes in the Changjiang River system: Sources effects and response to weathering and erosion. Geochim. Cosmochim. Acta 151, 117-132.

Wang, Y., Zhu, X., Mao, J., Cheng, Y., Li, Z., 2014. Preliminary study on Cu isotopic geochemistry behavior of Dongguashan Porphyry-skarn Deposit, Tongling District. Acta Geologica Sinica, 88(12), 2413-2422. (in Chinese with English abstract)

Wang, Z.L., Zhang, J., Liu, C.Q., 2007. Strontium isotopic compositions of dissolved and suspended loads from the main channel of the Yangtze River. Chemosphere 69(7), 1081-1088.

Wei, X., Hao, M., Shao, M., 2007. Copper fertilizer effects on copper distribution and vertical transport in soils. Geoderma 138(3), 213-220.

Weinstein, C., Moynier, F., Wang, K., Paniello, R., Foriel, J., Catalano, J., Pichat, S., 2011. Isotopic fractionation of Cu in plants. Chem. Geol. 286(3), 266-271.

Wells, M.L., Kozelka, P.B., Bruland, K.W., 1998. The complexation of `dissolved' Cu, Zn, Cd and Pb by soluble and colloidal organic matter in Narragansett Bay, RI. Mar. Chem. 62(3-4), 203-217.

Wu, W., Zheng, H., Xu, S., Yang, J., Liu, W., 2013. Trace element geochemistry of riverbed and suspended sediments in the upper Yangtze River. J. Geochem. Explor. 124, 67-78.

Xu, K., Milliman, J.D., 2009. Seasonal variations of sediment discharge from the Yangtze River before and after impoundment of the Three Gorges Dam. Geomorphology 104(3), 276-283.

Yan, J., Guo, X., Li, W., Jingyan, N., 2014. Determination of Heavy Metals in Fertilizer. Guangdong Chemical Industry, 41(01), 163-164. (in Chinese with English abstract)

Zhang, C., Wang, L., Zhang, S., Li, X., 1998. Geochemistry of rare earth elements in the mainstream of the Yangtze River, China. Appl. Geochem. 13(4), 451-462.

Zhang, M., Guo, X.M., Tian, B.Y., Wang, J., Qi, S.Y., Yang, Y.F., Xin, B.P., 2019. Improved bioleaching of copper and zinc from brake pad waste by low-temperature thermal pretreatment and its mechanisms. Waste Manage. 87, 629-635.

Zhang, Q., Ye, X., Werner, A.D., Li, Y., Yao, J., Li, X., Xu, C., 2014. An investigation of enhanced recessions in Poyang Lake: Comparison of Yangtze River and local catchment impacts. J. Hydrol. 517, 425-434.

Zhao, X.J., Gao, B., Xu, D.Y., Gao, L., Yin, S.H., 2017. Heavy metal pollution in sediments of the largest reservoir (Three Gorges Reservoir) in China: a review. Environ. Sci. Pollut. Res. 24(26), 20844-20858.

Zhu, X.K., O'Nions, R.K., Guo, Y., Belshaw, N.S., Rickard, D., 2000. Determination of natural Cu-isotope variation by plasma-source mass spectrometry: implications for use as geochemical tracers. Chem. Geol. 163(1), 139-149.

Figure captions

Fig. 1. The lithologic map and sampling sites of the Yangtze River drainage area. Modified from Ding et al. (2014). The green sites (Wuhan to Nanjing) and associated tributaries (white sites) were collected in September 2013; the red sites (Chongqing to Chibi) and associated tributaries (white sites) were collected at the end of July 2014. The abbreviations (blue for main channel, green for tributaries) in this figure correspond to the locations listed in Table 1. TGD means the Three Gorges Dam, with a sample site CJSX-01. GXZ-1 and LGT-1 represent Guangxingzhou and Leigutai, respectively. WHHJ-1 and CJHJ-1 overlapped in the figure represent the tributaries "Hanjiang" in Wuhan. JJ-1 and TL-1 represent Jiujiang and Tongling, respectively. Evaporitic rocks which are not marked in the figure can also be found in the Yangtze River basin (Chetelat et al., 2008).

Fig. 2. The concentrations of Ca and Mg in the Yangtze River mainstream water.

Fig. 3. δ^{65}Cu of the Yangtze River. The average mean and range of δ^{65}Cu in global rivers is referred from Vance et al. (2008); the data for Dongxiang and Dongguashan ore deposits are referred from Ouyang et al. (2017) and Wang et al. (2014), respectively.

Fig. 4. Riverine Cu isotope compositions plotted against Cu concentrations. The data of other world rivers are referred from Vance et al. (2008) and Guinoiseau et al.

(2018). New data for the main stream of the Yangtze River are shown in blue circles. The dashed line shows the Cu-δ^{65}Cu trend in the main stream of the Yangtze River.

Fig. 5. Molar Cu/Ca ratios for the dissolved load in the Yangtze River mainstream water.

Fig. 6. Plot of δ^{65}Cu vs. 1/Cu in the Yangtze River. An illustrative linear mixing line is shown between two hypothetical end-members (black diamonds); see text for details. Correlations (blue text) are calculated for the data of main channel only.

Fig. 7. The distribution of Cu deposits in the Yangtze River basin. The map of deposits is modified from information in: http://www.mining120.com/

Fig. 8. (a) The changes in pH (green circles) and Cu concentrations (orange diamonds) in the upper reaches of the Yangtze River. Inset (b) Correlation of pH and δ^{65}Cu for the upper reaches of the Yangtze River. Open symbols represent an outlier that is considered to be inaccurate.

Fig. 9. Cu isotope compositions plotted versus 1/Cu concentration. Model curves represent equilibrium partitioning of Cu between the dissolved and particulate phases in the main channel. The dashed curve represents the modeled evolution from a starting composition of the maximum measured Cu concentration (~100 nmol/L) and

lightest Cu isotope composition (+0.6‰). The solid curve represents the evolution from a starting pool of 40 nmol/L and +1‰, assuming that the three circled points are influenced by Cu supply from the weathering of Cu sulphide deposits. $\Delta_{diss-part}$ values give the modelled Cu isotopic fractionation between dissolved and particulate phases ($\delta^{65}Cu_{diss} - \delta^{65}Cu_{part}$) in each scenario. See text for full details.

Figure 1

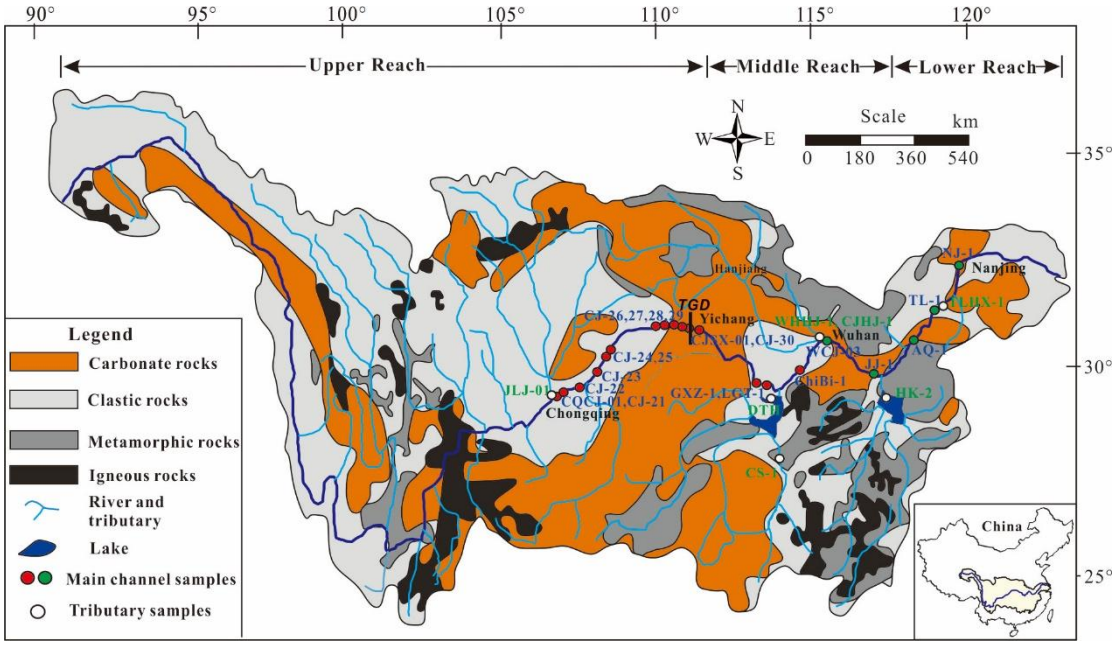

Figure 2

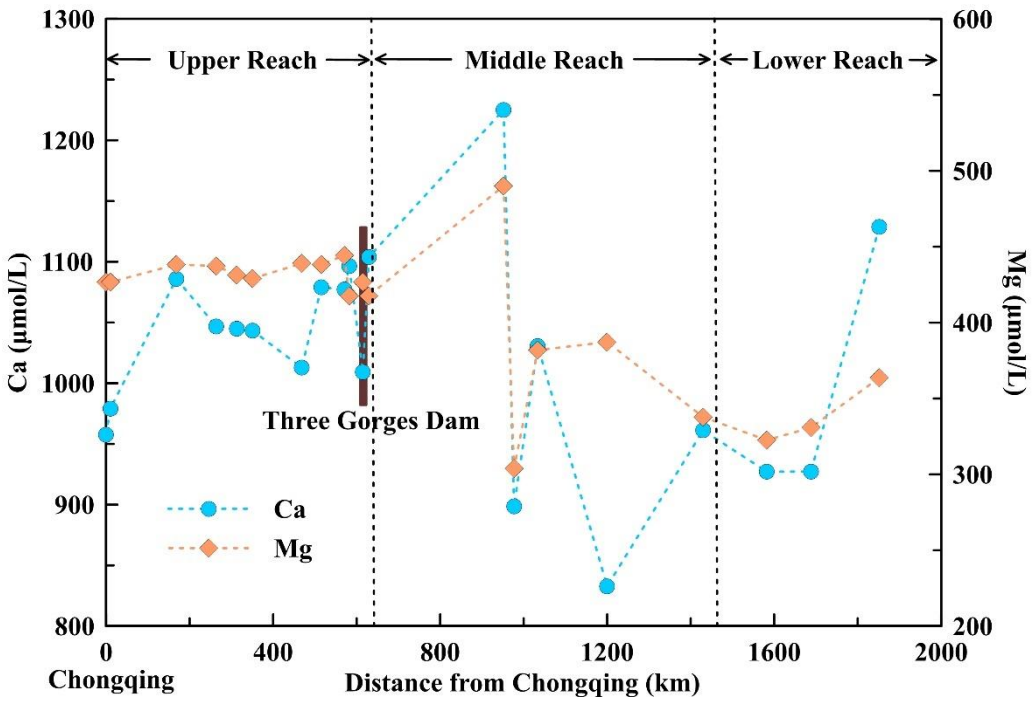

Figure 3

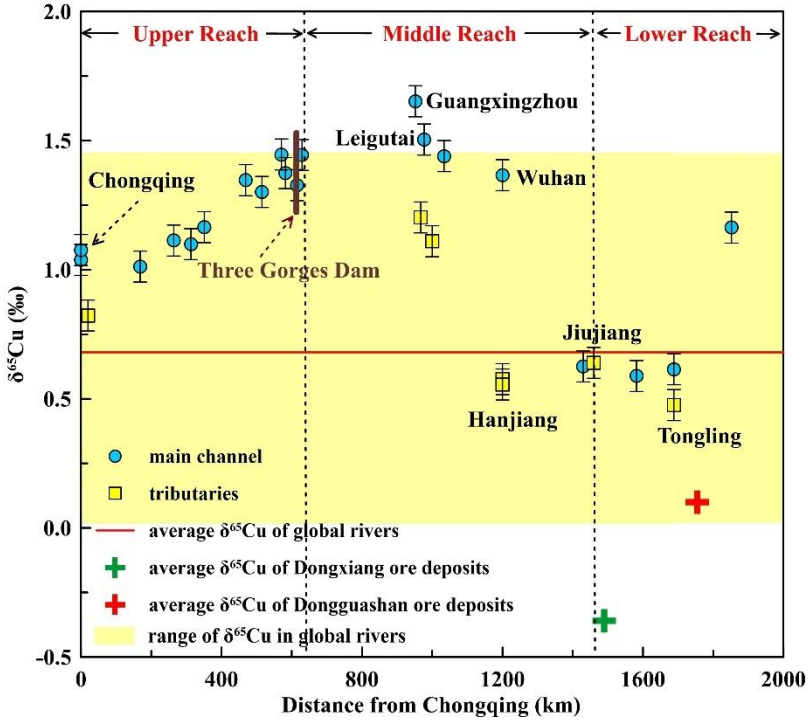

Figure 4

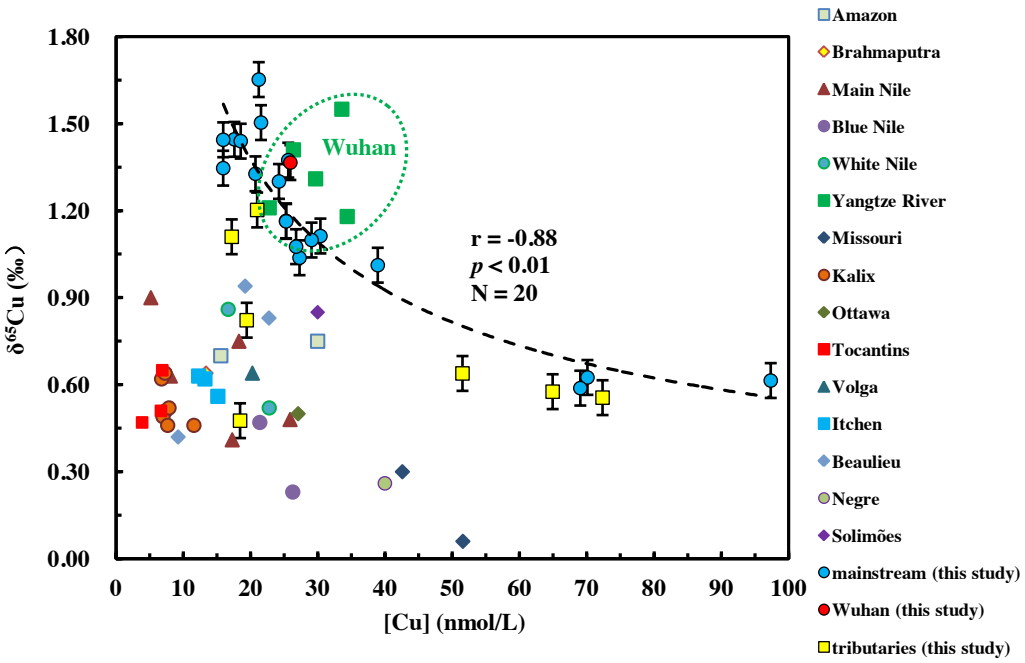

Figure 5

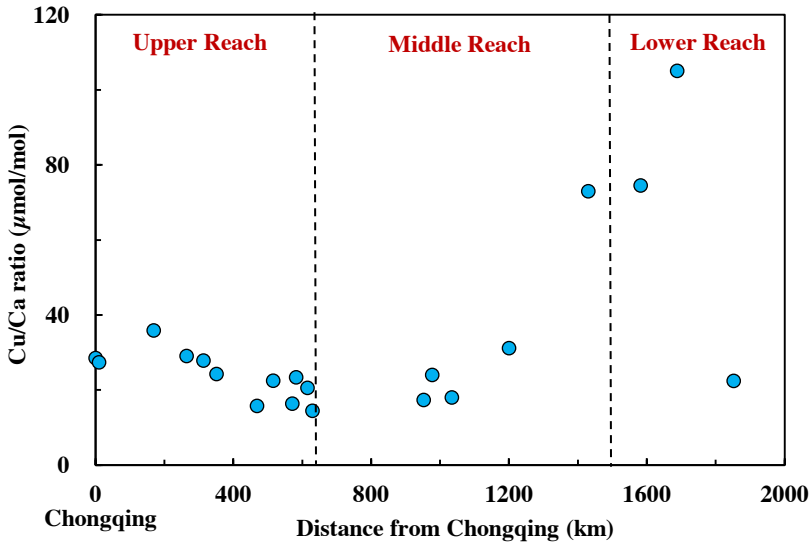

Figure 6

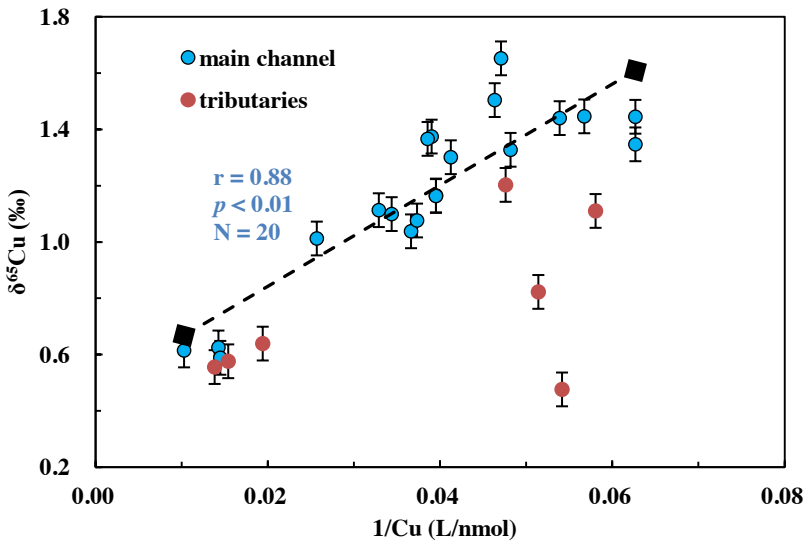

Figure 7

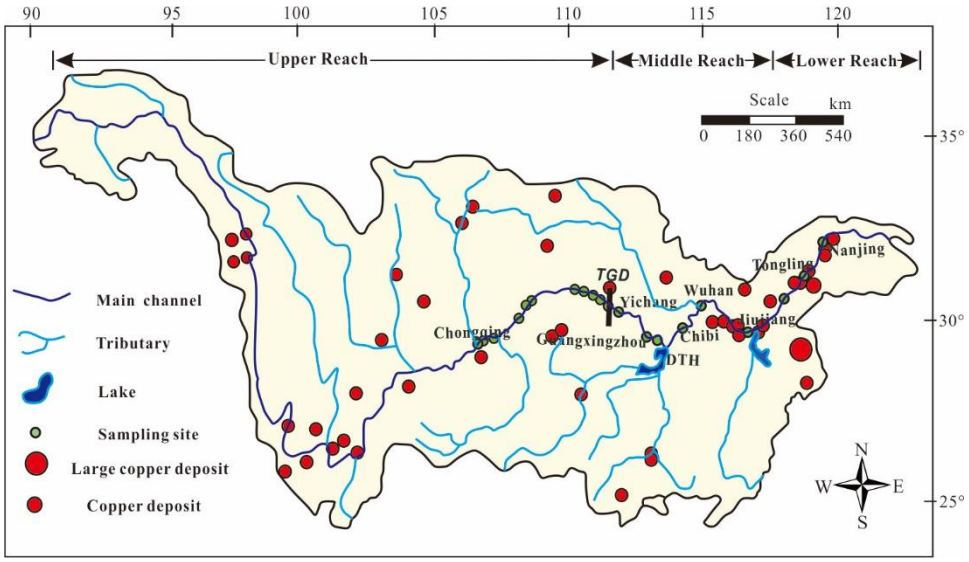

Figure 8

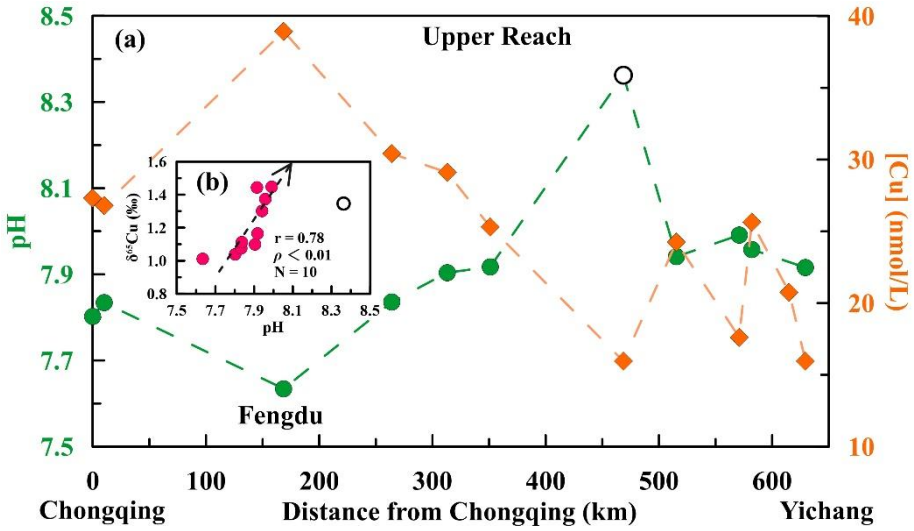
(a)
Upper Reach
Fengdu
pH
[Cu] (nmol/L)
Chongqing
Distance from Chongqing (km)
Yichang
(b)
δ65Cu (‰)
pH
r = 0.78
ρ < 0.01
N = 10

Figure 9

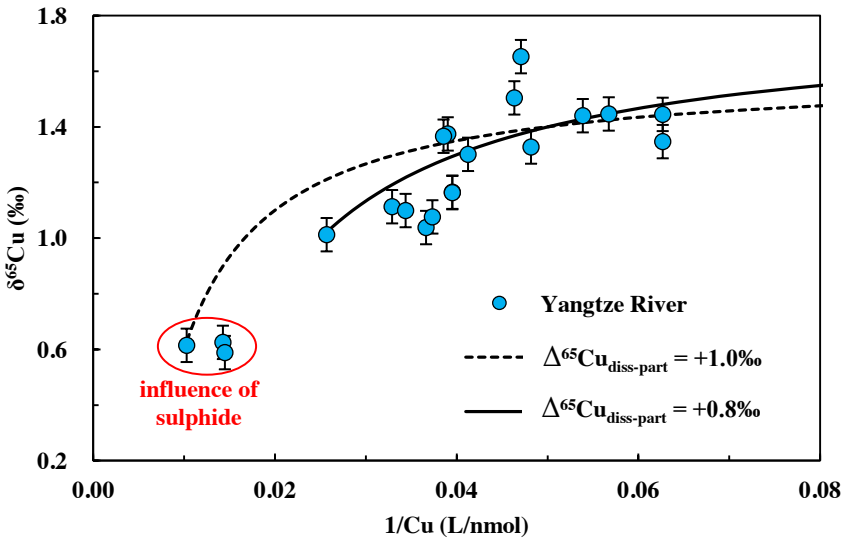
δ65Cu (‰)
1/Cu (L/nmol)
Yangtze River
Δ65Cudiss-part = +1.0‰
Δ65Cudiss-part = +0.8‰
influence of sulphide

Table 1

Data of dissolved components in the Yangtze River. The 2SD of $\delta^{65}Cu$ is the external reproducibility of repeated analysis from GPMR MC-ICP-MS.

	Sample	Location	Latitude (N)	Longitude (E)	Water discharge* (m^3/s)	Distance (km)	pH	EC ($\mu S \cdot cm^{-1}$)	D.O. (mg/L)	$\delta^{65}Cu$ (‰)	2 SD (‰)	$^{87/86}Sr$	2σ	Mg (μmol/L)	Ca (μmol/L)	Na (μmol/L)	Cu (nmol/L)	Sr (nmol/L)	P (nmol/L)
Main channel																			
1	CQCJ-01	Chongqing	29.542	106.539	19700	0	7.80	322	6.60	1.04	0.06	0.710722	12	427	958	462	27.3	2855	1476
2	CJ-21	Chongqing	29.654	106.601	19700	10	7.83	324	6.31	1.08	0.06	0.710728	10	427	979	442	26.8	3057	1151
3	CJ-22	Fengdu	29.548	107.725		169	7.63	341	5.06	1.01	0.06	0.710243	14	438	1086	421	38.9	3378	1710
4	CJ-23	Shibaozhai	30.417	108.189		264	7.84	337	6.61	1.11	0.06	0.710260	12	437	1047	427	30.4	3334	1307
5	CJ-24	Wanzhou	30.801	108.393		313	7.90	331	6.73	1.10	0.06	0.710273	14	431	1045	422	29.1	3308	867
6	CJ-25	Yunyangxian	30.932	108.676		351	7.92	331	7.07	1.16	0.06	0.710337	10	429	1043	421	25.3	3312	1004
7	CJ-26	Wushan	31.076	109.885		469	8.36	337	7.35	1.35	0.06	0.710194	10	439	1013	465	16.0	3408	741
8	CJ-27	Badong	31.044	110.324		515	7.94	346	7.20	1.30	0.06	0.710279	14	438	1079	444	24.2	3398	933
9	CJ-28	Xiangxizhen	30.962	110.743		571	7.99	347	7.24	1.45	0.06	0.710230	12	444	1077	458	17.6	3477	931
10	CJ-29	Taipingxi	30.851	110.998		582	7.96	350	7.09	1.37	0.06	0.710159	12	418	1097	466	25.6	3361	601
11	CJSX-01	the Three Gorges Dam	30.825	111.006		615	-	-	-	1.33	0.06	0.710488	12	427	1009	2996	20.8	3569	3561
12	CJ-30	Yichang	30.683	111.299	27100	629	7.92	351	7.37	1.44	0.06	0.710158	12	418	1104	459	16.0	3100	490
13	GXZ-1	Guangxingzhou	29.550	112.920		952	8.04	404	8.64	1.65	0.06	0.709923	14	490	1225	608	21.2	4865	4085
14	LGT-1	Leigutai	29.507	113.192		977	7.76	274	7.75	1.50	0.06	0.711139	12	304	899	315	21.6	1924	1381
15	ChiBi-1	Chibi	29.886	113.618		1034	7.98	329	8.64	1.44	0.06	0.710345	12	382	1031	422	18.6	3013	2005
16	WCJ-03	Wuhan	30.554	114.291	21900	1200	8.25	340	-	1.37	0.06	0.710650	12	387	833	4175	25.9	2876	4801
17	JJ-1	Jiujiang	29.742	116.008		1430	7.78	293	-	0.63	0.06	0.710661	12	338	961	424	70.1	2462	3919
18	AQ-1	Anqing	30.500	117.039		1582	7.84	285	-	0.59	0.06	0.710802	14	323	927	431	69.1	2274	3872
19	TL-1	Tongling	30.926	117.763	25100	1688	7.69	290	-	0.61	0.06	0.710778	10	331	927	442	97.4	2283	4516
20	NJ-1	Nanjing	32.050	118.767		1852	-	-	-	1.16	0.06	0.710388	12	364	1129	431	25.3	3403	1434
Tributaries																			
21	JLJ-01	Jialingjiang	29.559	106.532	2640	20	7.63	351	6.55	0.82	0.06	0.710656	10	462	1155	376	19.5	4307	977
22	CS-1	Xiangjiang	28.203	112.968	1330	1000	-	-	-	1.11	0.06	0.712057	10	424	997	442	17.2	993	791
23	DTH	Dongtinghu	29.373	113.092		967	7.76	254	7.75	1.20	0.06	0.711397	10	280	827	305	21.0	1622	1393
24	WHHJ-1	Hanjiang (center)	30.569	114.281	410	1200	8.04	360	-	0.58	0.06	0.710309	12	393	1095	636	64.9	1972	3146
25	CJHJ-1	Hanjiang (junction)	30.566	114.286	410	1200	7.99	343	-	0.56	0.06	0.710899	12	383	1057	532	72.4	2373	3632
26	HK-2	Poyanghu	29.747	116.209		1460	7.37	148	-	0.64	0.06	0.715410	14	131	366	385	51.5	647	1361
27	TLHX-1	Hongxing River	30.943	117.866		1688	7.54	709	-	0.48	0.06	0.708655	12	632	3022	533	18.5	16677	3236

*The discharge was recorded from the web of the hydrological information for the main rivers in China (http://xxzx.mwr.gov.cn/).

Table 2

δ^{65}Cu (‰) and 2SD for three USGS reference materials compared to recommended values

	δ^{65}Cu	2SD	n	References
BHVO-2	0.13	0.05	7	This study
	0.12	0.02	-	Moynier et al., 2017
BCR-2	0.21	0.02	4	This study
	0.17	0.05	-	Moynier et al., 2017
GSP-2	0.27	0.01	3	This study
	0.30	0.04	-	Liu S. et al., 2014

Table 3

Cu concentrations and δ^{65}Cu in different sources

Site	Sample type	Cu concentration (μg/g)	Cu concentration (ng/m^3)	δ^{65}Cu (‰)	± 2SD	Reference
close to Marylebone and North Kensington	Brake	6.1		0.62	0.13	Dong et al., 2017
		4.4		0.63	0.14	
	Tire	25		0.28	0.1	
		43		0.27	0.09	
		41		0.17	0.1	
		26		0.33	0.12	
North Kensington	PM_{10}		1.9 ~ 3.6	-0.01 ~ +0.46		Dong et al., 2017
Marylebone Road	PM_{10}		9.4 ~ 130	+0.01 ~ +0.51		

Figure
Click here to download high resolution image

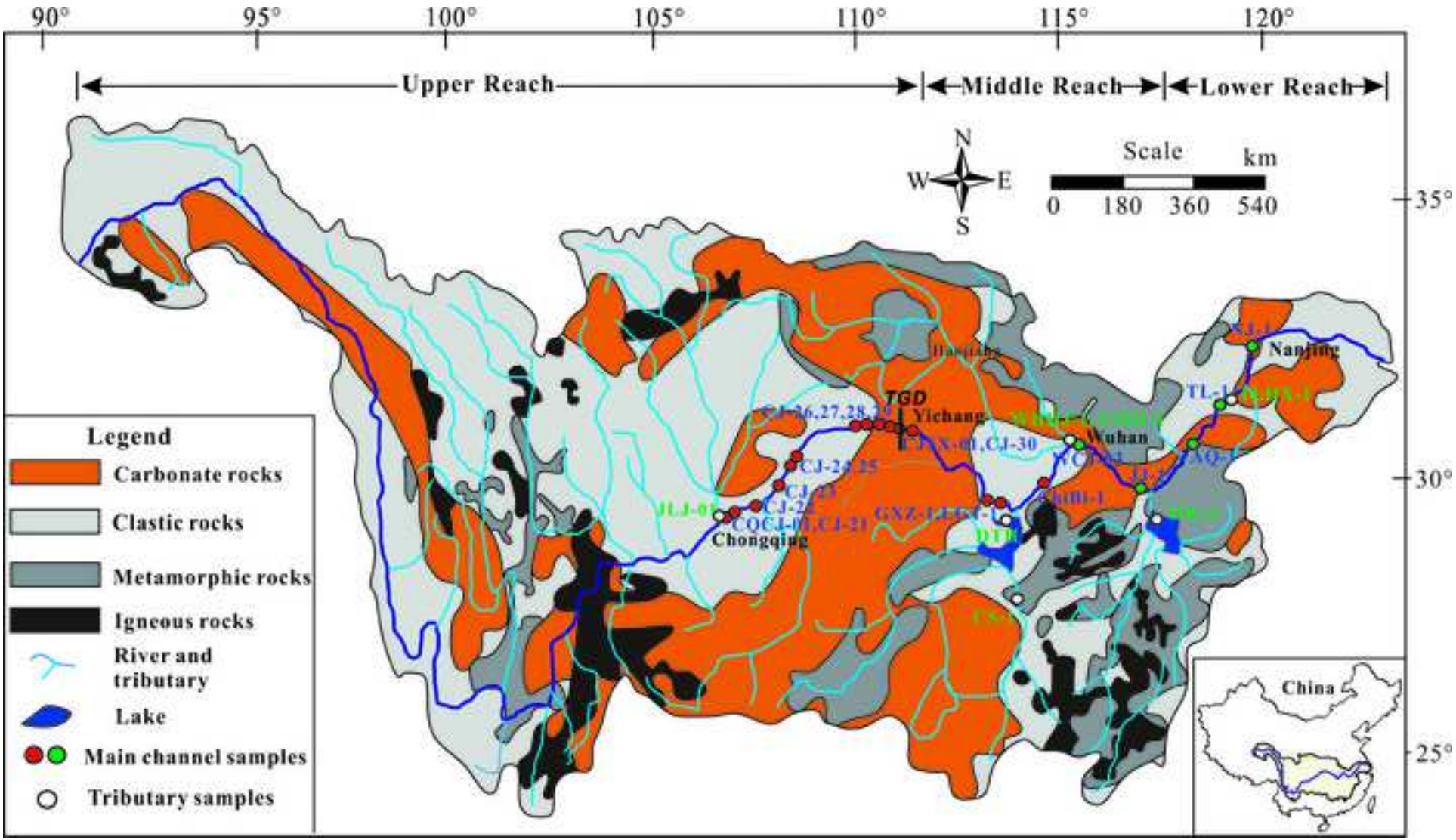

Figure
Click here to download high resolution image

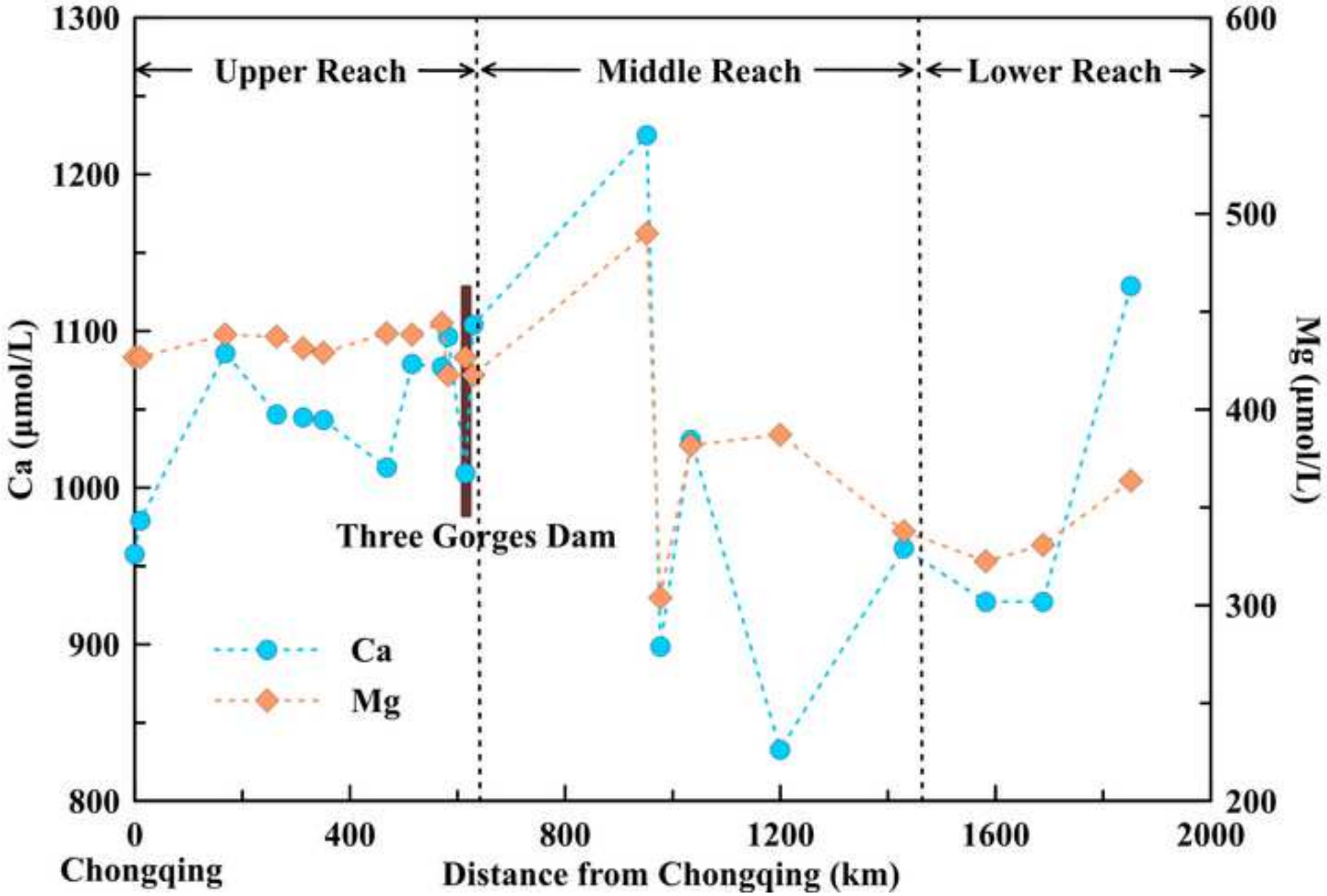

Figure
Click here to download high resolution image

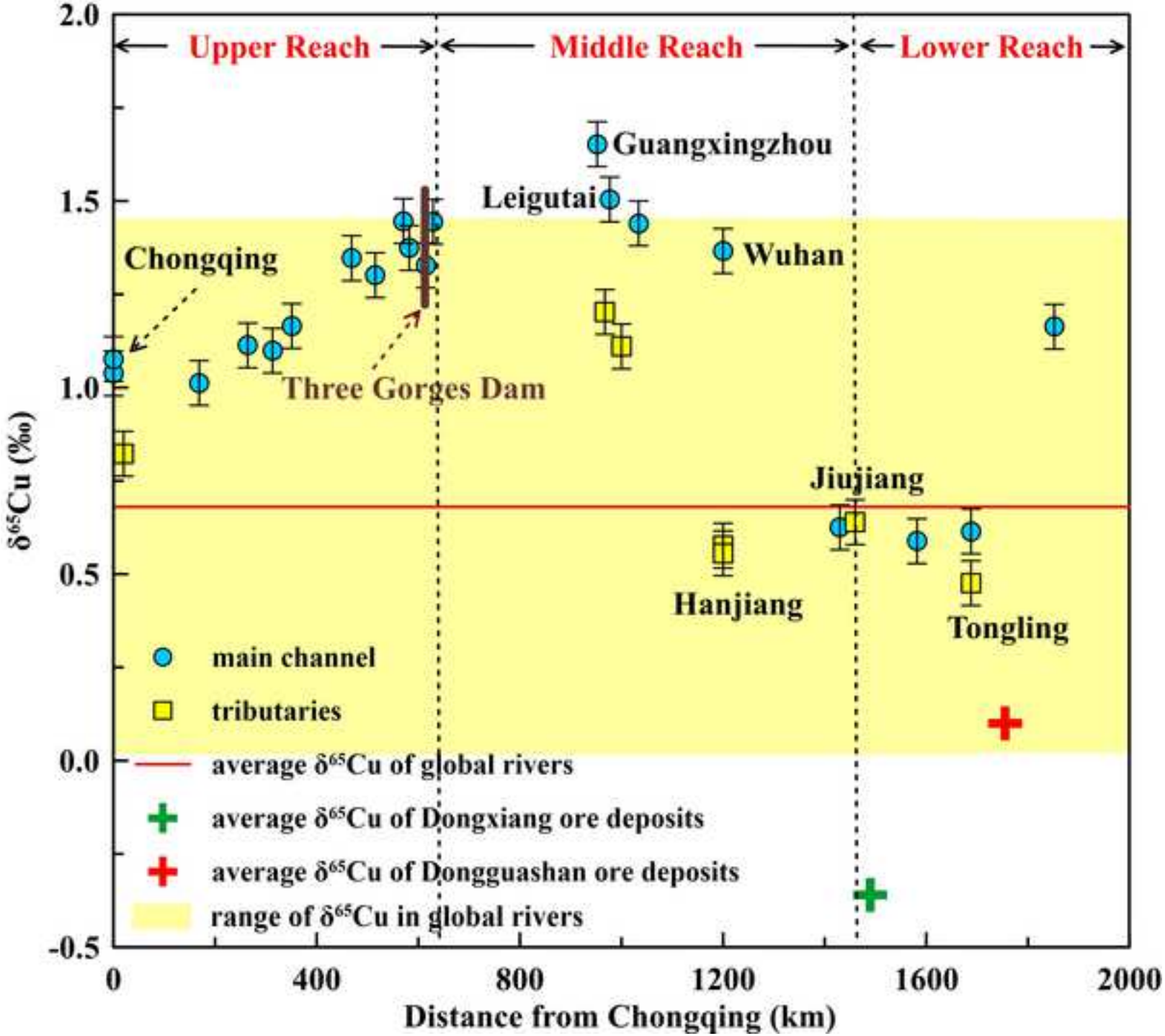

Figure
Click here to download high resolution image

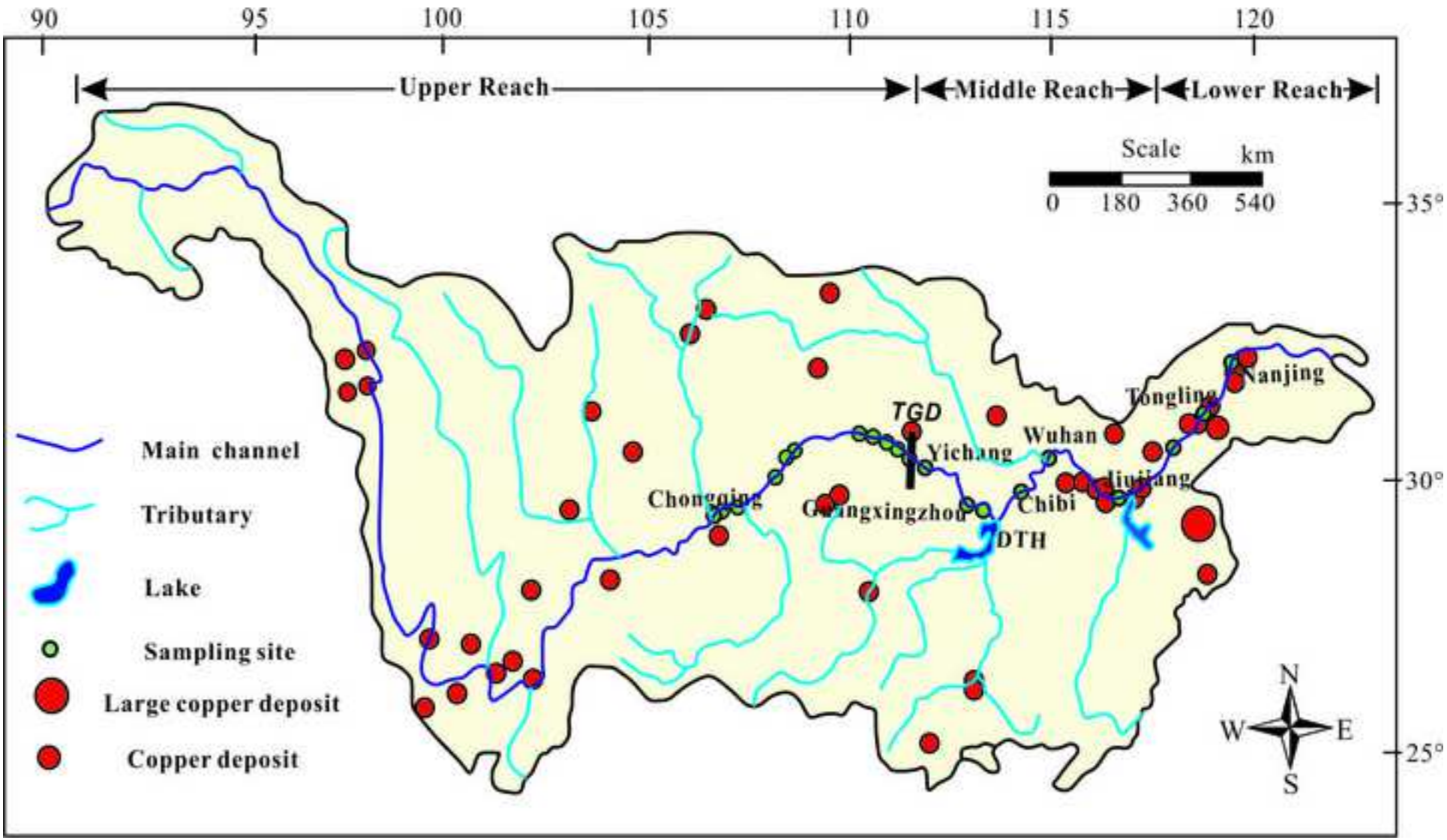

Figure
Click here to download high resolution image

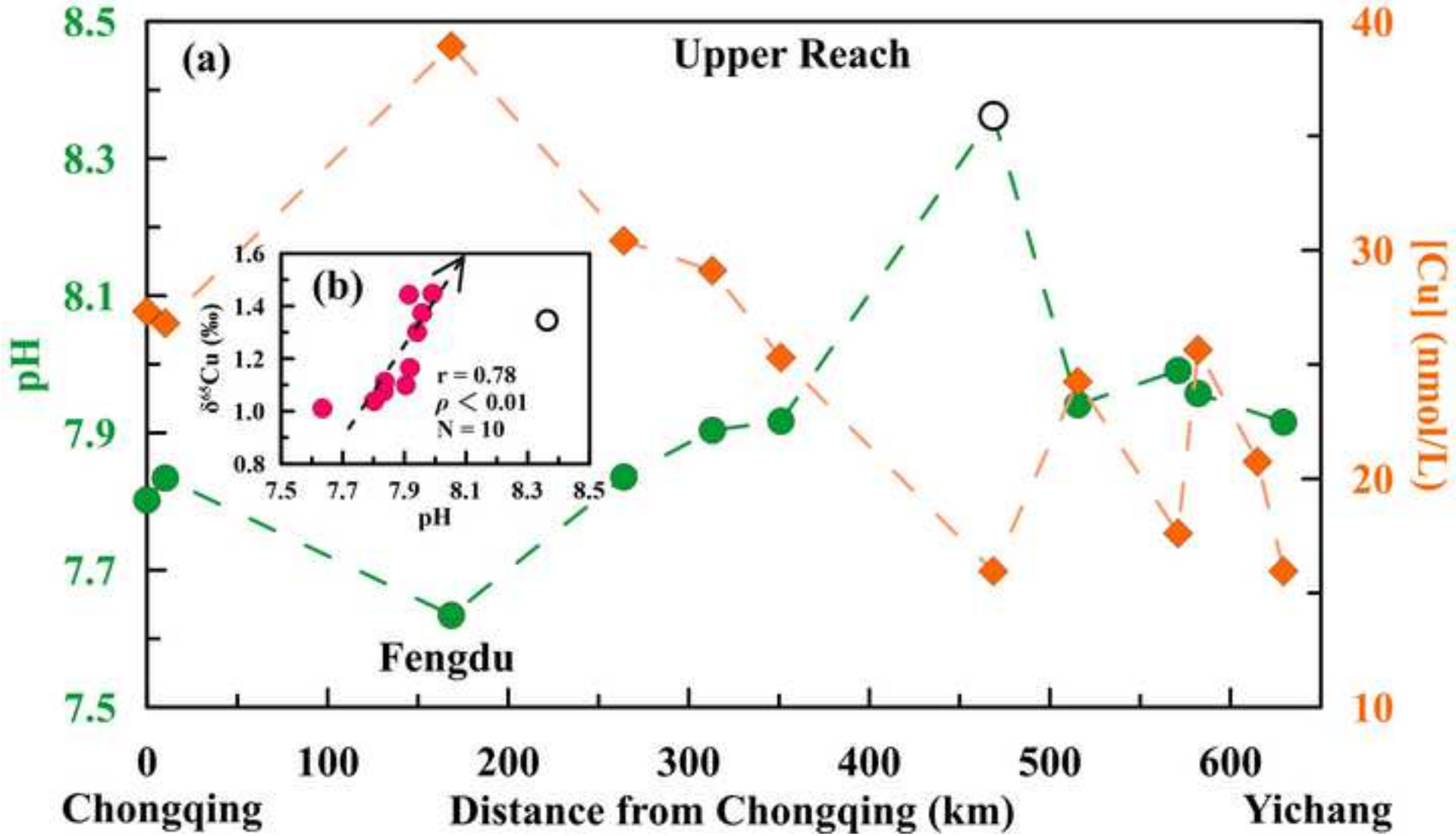

***conflict of Interest Statement**

Declaration of interests

☒ The authors declare that they have no known competing financial interests or personal relationships that could have appeared to influence the work reported in this paper.

☐The authors declare the following financial interests/personal relationships which may be considered as potential competing interests:

No

***Credit Author Statement**

Qian Wang: Methodology, Formal analysis, Investigation, Data Curation, Writing - Original Draft; **Lian Zhou:** Conceptualization, Methodology, Resources, Writing - Review & Editing, Supervision, Project administration, Funding acquisition; **Susan H. Little:** Methodology, Formal analysis, Writing - Review & Editing; **Jinhua Liu:** Investigation, Data Curation; **Lanping Feng:** Investigation; **Shuoyun Tong:** Investigation